A selection of mathematical topics in multiscale sciences

Claude Le Bris

École Nationale des Ponts et Chaussées, 6 & 8, avenue Blaise Pascal, 77455 Marne-La-Vallée Cedex 2,

INRIA Rocquencourt, MICMAC project-team, Domaine de Voluceau, B.P. 105, 78153 Le Chesnay Cedex, FRANCE.

lebris@cermics.enpc.fr

Abstract

We present here some basic elements of the mathematical theory for three different contexts of multiscale simulation: homogenization theory for elliptic equations, atomistic to continuum models for elastic materials, and micro-macro models for polymeric fluids. The exposition is pedagogic and elementary. Both theoretical and numerical aspects are addressed.

1 Introduction

We present here some basic elements of the mathematical theory for multiscale simulation in three different contexts: homogenization theory for linear elliptic equations in Sections 2, 3, and 4, atomistic to continuum models for elastic materials in Section 5, and micro-macro models for polymeric fluids in Section 6. The exposition is pedagogic and elementary. Both theoretical and numerical aspects are addressed. The material contained in these lectures notes is adapted from several publications of the author, some of them in co-authorship: the textbook [117] (in French) for the basic theory of homogenization, the works [40, 64, 116, 32] for more advanced aspects –in particular related to stochastic homogenization–, the review articles [42, 123] for multiscale simulations of solids and fluids. Many other references are mentioned in the body of the text.

Of course, these lectures notes are only a poor surrogate to more extensive presentations contained in well known textbooks and monographs. This is especially true for Sections 2 and 3 where we present basic elements that may be found in many places in the literature. We by no means claim for originality, except, perhaps, for having collected in a single set of notes topics different in nature that are (to the best of the author's knowledge) nowhere addressed in a unified and elementary manner. Even periodic homogenization and stochastic homogenization are not often covered simultaneously. For more detailed views on the topics, we refer, for instance to [28, 58, 99, 4] for homogenization, [151, 153] for multiscale fluid modelling.

A more comprehensive presentation of some more advanced topics hardly approached in the first three sections in homogenization theory will be given in two publications in preparation [118, 119].

2 Periodic Homogenization

Our first topic is homogenization, and we begin by a short simple exposition of a prototypical problem in the periodic setting. The purpose of this Section 2 is then to recall some basic ingredients of elliptic homogenization theory in the periodic setting. We refer *e.g.* to the monographs [28, 58, 99] for more details on homogenization theory, to [4, Chapters 1 and 2] for a pedagogic introduction, and to [97] for a short non technical overview of related problems.

We consider, in a regular bounded domain $\mathcal{D}$ in $\mathbb{R}^d$, the problem

$$\left\{ \begin{array}{l} -\mathrm{div}\left[A_{per}\left(\frac{x}{\varepsilon}\right)\nabla u^\varepsilon\right] = f \quad \text{in} \quad \mathcal{D}, \\ \\ u^\varepsilon = 0 \quad \text{on} \quad \partial\mathcal{D}, \end{array} \right. \tag{2.1}$$

where the matrix A_{per} is $\mathbb{Z}^d$-periodic and (for simplicity) symmetric. In order to ensure well-posedness, we assume the *coercivity* condition: $(A(y)z, z) \geq c\|z\|^2$ for some $c > 0$ independent from $z \in \mathbb{R}^d$ and $y \in Q$. For ε small, the above problem is prohibitively expensive to treat computationally: the typical meshsize to use in a finite element method (say) must be smaller than ε in order to capture the oscillations of the solution u^ε arising from the oscillations of the coefficient $A_{per}\left(\frac{x}{\varepsilon}\right)$. The purpose of homogenization is to replace

problem (2.1) by an equivalent, a.k.a. *homogenized*, problem, the solution $u^\star$ of which is close to u^ε for ε sufficiently small, in a sense made precise below. The first step of the construction of the homogenized problem, as will be shown in the following sections, is the solution to the so-called *corrector problem* associated to (2.1) which reads, for p fixed in $\mathbb{R}^d$,

$$\begin{cases} -\mathrm{div}\left(A_{per}(y)\left(p+\nabla w_p\right)\right)=0, \\ \\ w_p \text{ is } \mathbb{Z}^d\text{-periodic.} \end{cases} \tag{2.2}$$

Problem (2.2) has a unique solution up to the addition of a constant. Then, the homogenized coefficients read

$$[A^\star]_{ij}=\int_Q \left(e_i+\nabla w_{e_i}(y)\right)^T A_{per}(y)\left(e_j+\nabla w_{e_j}(y)\right)dy=\int_Q \left(e_i+\nabla w_{e_i}(y)\right)^T A_{per}(y)e_j dy, \tag{2.3}$$

where $Q=[0,1]^d$ is the unit cube. The main result of periodic homogenization theory is that, as ε goes to zero, the solution u^ε to (2.1) converges to $u^\star$ solution to

$$\begin{cases} -\mathrm{div}\left[A^\star\nabla u^\star\right]=f \quad \text{in} \quad \mathcal{D}, \\ \\ u^\star=0 \quad \text{on} \quad \partial\mathcal{D}. \end{cases} \tag{2.4}$$

The convergence holds in $L^2(\mathcal{D})$, and weakly in $H_0^1(\mathcal{D})$. The correctors w_{e_i} (for e_i the canonical vectors of $\mathbb{R}^d$) may then also be used to "correct" $u^\star$, that is, identify the behavior of u^ε in the strong topology $H_0^1(\mathcal{D})$. Several other convergences involving $A_{per}\left(\dfrac{x}{\varepsilon}\right)$ and u^ε also hold. All this is well documented.

The practical interest of the approach is evident. No small scale ε is present in the homogenized problem (2.4). At the price of only computing d periodic problems (2.2) (as many problems as dimensions in the ambient space, taking indeed p the vectors of the canonical basis of $\mathbb{R}^d$), the solution to problem (2.1) can be efficiently approached for ε small. As above mentioned, a direct attack of problem (2.1) would require taking a meshsize smaller than ε. The difficulty has been circumvented.

We will now take a pedestrian approach that explains why the above result hold. We will examine the related numerical techniques in Section 3.

2.1 "Zero-dimensional" intuition

To begin with, we modify (2.1) in a dramatic way: we consider a one-dimensional domain, take A_{per} a scalar valued function (denoted a_{per} for simplicity), delete the differential operators of (2.1), and are left with the oversimplified equation $-a_{per}\left(\frac{x}{\varepsilon}\right) u^\varepsilon(x) = f(x)$, which admits the obvious solution

$$u^\varepsilon(x) = -a_{per}^{-1}\left(\frac{x}{\varepsilon}\right) f(x)\,. \tag{2.5}$$

We see that finding an homogenized problem then amounts to identifying the behaviour, as ε vanishes, of the sequence of oscillating functions $a_{per}^{-1}\left(\frac{x}{\varepsilon}\right)$.

The topology of *weak convergence* is the appropriate tool for this purpose.

Proposition 1. *Let b be a function in $L^\infty(\mathbb{R})$, assumed 1- periodic. Then the sequence of functions $b(\frac{\cdot}{\varepsilon})$ weakly-$\star$ converges in $L^\infty(\mathbb{R})$ to the constant function with value $< b >$, called the* average *of b:*

$$< b >= \int_0^1 b. \tag{2.6}$$

Recall that a sequence of functions f_n is said to weakly-$\star$ converge in $L^\infty(\mathbb{R})$ to f_∞, if for all functions $g \in L^1(\mathbb{R})$, $\int f_n\, g$ converges to $\int f\, g$.

Proof of Proposition 1:

For consistency, we outline the simple proof of Proposition 1. We wish to prove that, for all $v \in L^1(\mathbb{R})$,

$$\int b(\frac{x}{\varepsilon}) v(x)\, dx \longrightarrow \int_0^1 b \int v.$$

It suffices to prove the claim when v is the characteristic function of an interval and then to use the density of piecewise constant functions in $L^1(\mathbb{R})$. For $\alpha < \beta$, we would like to prove that

$$\int_\alpha^\beta b(\frac{x}{\varepsilon})\, dx \longrightarrow (\beta - \alpha) \int_0^1 b.$$

Using periodicity and denoting by $[x]$ the integer part of the scalar x, we have

$$\begin{aligned}
\int_\alpha^\beta b(\frac{x}{\varepsilon})\, dx &= \varepsilon \int_{\frac{\alpha}{\varepsilon}}^{\frac{\beta}{\varepsilon}} b(y)\, dy \\
&= \varepsilon([\frac{\beta}{\varepsilon}] - [\frac{\alpha}{\varepsilon}] - 1) < b > + \varepsilon \int_{\frac{\alpha}{\varepsilon}}^{[\frac{\alpha}{\varepsilon}]+1} b(y)\, dy + \varepsilon \int_{[\frac{\beta}{\varepsilon}]}^{\frac{\beta}{\varepsilon}} b(y)\, dy \\
&= (\beta - \alpha) < b > + O(\varepsilon).
\end{aligned} \tag{2.7}$$

This concludes the proof. ♢

Remark 1. *The result of Proposition* 1 *of course holds true in any dimension. The proof can be indeed easily adapted to the multidimensional setting.*

Considering Proposition 1, we obtain

$$u^\star = -\langle a_{per}^{-1}\rangle\, f\,, \tag{2.8}$$

as the weak-$\star$ limit of u^ε in (2.5) when ε vanishes. Based on this, it is natural to guess that the homogenized equation arising from (2.1) will be related to the average of the periodic function A_{per}^{-1}. We will see that it is indeed the case, at least in the one-dimensional setting.

We remark that an even more naïve approach would consist, given the statement of Proposition 1, in guessing that the homogenized equation is obtained, as ε vanishes, by simply replacing in (2.1) $A_{per}\left(\frac{x}{\varepsilon}\right)$ by its average $\langle A_{per}\rangle$. This is *not* correct, as will be seen in the simple one-dimensional setting in the next section. It is actually already clear on our "zero-dimensional" calculation, since we obtain (2.8) and *not*: $u^\star = -\left(\langle a_{per}\rangle\right)^{-1} f$. Unless the function is constant, we never have $\langle b^{-1}\rangle = \left(\langle b\rangle\right)^{-1}$ (see a proof below). Otherwise stated, knowing the statistics of A_{per} is not sufficient to know the statistics on the solution u, and this of course owes to the fact that the map $A_{per} \longrightarrow u$ that associates to A_{per} the solution u to the equation is *not* linear.

2.2 One-dimensional setting

We now reinstall the differential operators, and consider the one-dimensional setting:

$$\left\{\begin{array}{rcl} -\dfrac{d}{dx}\left(a\left(\dfrac{x}{\varepsilon}\right)\dfrac{d}{dx}u^\varepsilon\right) &=& f, \quad \text{in }]0,1[\\ \\ u^\varepsilon(0) = u^\varepsilon(1) &=& 0, \end{array}\right. \tag{2.9}$$

where a is a 1-periodic, scalar valued function. We assume it is positive, bounded and bounded away from zero, that is, there exist $0 < c_1 \leq c_2 < +\infty$ such that

$$0 < c_1 \leq a(x) \leq c_2\,, \quad \forall x \in]0,1[. \tag{2.10}$$

We additionally assume that $f \in L^2(]0,1[)$.

Consider u^ε the solution to (2.9). For brevity, we omit to prove here that u^ε uniquely exists. This is evident, either *solving* the equation (recall we are working in one dimension !), or using the Lax-Milgram lemma (and then the proof of course carries over to the multidimensional setting). An alternative to the latter approach, which then can be adapted to cover the case of dimensions higher than or equal to 2 and *provided* the matrix A_{per} is symmetric, is to remark that the equation considered is indeed the Euler-Lagrange equation associated to the minimization in $H^1_0(]0,1[)$ of the strongly convex energy functional $\frac{1}{2}\int_0^1 a(\frac{x}{\varepsilon})|\frac{dv}{dx}|^2 - \int_0^1 fv$. We will return to this interpretation in Section 2.6.

We now prove

Proposition 2. *The solution $u^\varepsilon \in H^1_0(]0,1[)$ to problem* (2.9) *converges in $L^2(]0,1[)$, and weakly in $H^1_0(]0,1[)$, to the solution $u^\star \in H^1_0(]0,1[)$ of the* homogenized *equation*

$$\frac{d}{dx}\left(\frac{1}{< a^{-1} >}\frac{d}{dx}u^\star\right) = f\,. \tag{2.11}$$

Proof of Proposition 2

We could of course prove the Proposition solving explicitly for u^ε solution to (2.9) and using its explicit expression. We shall indeed make use of the explicit expression of the solution u^ε later on (see Section 2.5). With a view to generality, we prefer to argue here without making use of any explicit expression of the solution. The proof is then closer to the proof needed in the multidimensional context (although it is still simpler).

Multiplying the equation by u^ε, integrating over the interval $[0,1]$ and integrating by parts, we obtain

$$\int_0^1 a(\frac{x}{\varepsilon})|\frac{d}{dx}u^\varepsilon|^2 = \int_0^1 f\,u^\varepsilon,$$

which, using the Cauchy-Schwarz inequality and the coercivity, yields

$$c_1\|\frac{d}{dx}u^\varepsilon\|^2_{L^2(]0,1[)} \leq \int_0^1 a(\frac{x}{\varepsilon})|\frac{d}{dx}u^\varepsilon|^2 \leq \|f\|_{L^2(]0,1[)}\|u^\varepsilon\|_{L^2(]0,1[)}.$$

Since u^ε vanishes at 0 and 1, we use the Poincaré inequality to obtain, for some constant $c > 0$,

$$c\|u^\varepsilon\|^2_{L^2(]0,1[)} \leq \|f\|_{L^2(]0,1[)}\|u^\varepsilon\|_{L^2(]0,1[)}.$$

The sequence u^ε and the sequence $\frac{d}{dx}u^\varepsilon$ are therefore both bounded in $L^2(]0,1[)$, that is, u^ε is bounded in $H^1_0(]0,1[)$. Using the Rellich Kondrakov theorem, we may assume, up

to the extraction of a subsequence, that u^ε converges in L^2 to some function $u^\star$, and that $\frac{d}{dx}u^\varepsilon$ weakly converges in L^2 to $\frac{d}{dx}u^\star$. By construction, $u^\star \in H^1_0(]0,1[)$.

The above part of the argument (establishment of *a priori* estimates and convergence up to an extraction) carries over to the multidimensional setting. The sequel of the proof now specifically exploits the one-dimensional setting in order to identify the limit.

We now integrate once (2.9):

$$-a(\frac{x}{\varepsilon})\frac{d}{dx}u^\varepsilon = \int_0^x f + c_\varepsilon, \tag{2.12}$$

where, using the bounds on a and u^ε, we know that the sequence of scalars c_ε is bounded. Up to an extraction, we may assume that c_ε converges to some c. We write

$$-\frac{d}{dx}u^\varepsilon = a^{-1}(\frac{x}{\varepsilon})\big(\int_0^x f + c_\varepsilon\big). \tag{2.13}$$

Since a^{-1} is also in L^∞ and periodic, we may apply Proposition 1, and we therefore know that $-\frac{d}{dx}u^\varepsilon$ weakly converges in L^2 to the function $< a^{-1} > \big(\int_0^x f + c\big)$. Hence

$$-\frac{d}{dx}u^\star =< a^{-1} > \big(\int_0^x f + c\big). \tag{2.14}$$

The limit $u^\star$ of the sequence u^ε of solutions to (2.9) therefore solves

$$-\frac{d}{dx}(\frac{1}{< a^{-1} >}\frac{d}{dx}u^\star) = f, \tag{2.15}$$

supplied with the boundary conditions $u^\star(0) = u^\star(1) = 0$. We finally note that, for another converging extraction of the sequence u^ε, we would obtain the same limit function and same limit equation, because the entire sequence $a^{-1}(\frac{\cdot}{\varepsilon})$ converges to $< a^{-1} >$, and the solution to (2.15) is unique. Thus our argument holds for the whole sequence itself, without any extraction needed. This concludes the proof. ♢

Remark 2. *We have already noticed, in the body of the proof, that the first part of the argument is not specific to the one-dimensional setting. We also note that this first part does not make use of the specific assumption put on the coefficient of the equation, namely here the periodicity. Only the second part of the argument uses the periodicity to explicitly identify the limit equation. This observation is not restricted to the one-dimensional setting (see Section* 2.7*).*

2.3 A striking numerical observation

We are now in position to demonstrate that naïvely using a discretization approach on a problem of type (2.1) leads to a *wrong* result when one cannot afford taking sufficiently fine discretization parameters. For this purpose, we consider the one-dimensional problem (2.9) and use a classical P1-finite element approach on a regular mesh of size $h \gg \varepsilon$ to mimick a difficult situation. The discrete variational formulation is set on the finite dimensional space $V_{0h} \subset H^1_0(]0,1[)$ of P1 finite elements and reads: *Find* $u_h^\varepsilon \in V_{0h}$ *such that, for all* $v_h \in V_{0h}$,

$$\int_0^1 a(\frac{x}{\varepsilon}) \frac{du_h^\varepsilon}{dx} . \frac{dv_h}{dx}\, dx = \int_0^1 f(x)\, v_h(x)\, dx. \tag{2.16}$$

The rigidity matrix $\mathcal{A}_h$ of the problem has entries

$$[\mathcal{A}_h]_{ij} = \int a(\frac{x}{\varepsilon})\, \phi_i'(x)\, \phi_j'(x)\, dx, \tag{2.17}$$

where we denote by ϕ_i a generic P1 finite element basis function. Proposition 1 tells us that, as ε goes to zero, these entries converge to

$$[\mathcal{A}_0]_{ij} = < a > \int \phi_i'(x)\, \phi_j'(x)\, dx. \tag{2.18}$$

These are indeed the entries of the rigidity matrix associated to the discrete variational formulation: *Find* $u_h \in V_{0h}$ *such that, for all* $v_h \in V_{0h}$,

$$< a > \int_0^1 \frac{du_h}{dx} . \frac{dv_h}{dx}\, dx = \int_0^1 f(x)\, v_h(x)\, dx, \tag{2.19}$$

which is the formulation associated, using the same discretization approach, to the differential equation

$$\left\{ \begin{array}{rcl} -< a > \dfrac{d^2}{dx^2} u & = & f, \quad \text{in }]0,1[\\ \\ u(0) = u(1) & = & 0. \end{array} \right. \tag{2.20}$$

Consequently, for a meshsize $h \gg \varepsilon$, the discrete finite element solution ressembles the solution to (2.20) and not that to the *correct* homogenized problem (2.11), unless the coefficient a is constant. Recall indeed that $< a^{-1} > = < a >^{-1}$ if and only if we have equality in the Cauchy-Schwarz inequality

$$\int 1 = \int \frac{1}{\sqrt{a}} \sqrt{a} \leq \left(\int a^{-1} \int a \right)^{1/2},$$

which imposes that a and a^{-1} are two proportional functions, and thus that a is constant.

We conclude that using too coarser a mesh on a problem with highly oscillating coefficients such as (2.9) for ε small is inappropriate. The purpose of homogenization is to bypass this difficulty.

2.4 Dimension 2 and beyond

It is now time to address the dimensions higher than or equal to two. The tremendous additional difficulty is that *geometry* comes into play.

Two exactly solvable settings

There are actually two particular settings known in dimension higher than one that still lead to an explicitly solvable homogenized problem: laminated materials and checkerboard materials. Let us briefly mention these two settings. They are useful both for theoretical considerations (they illustrate how much the two-dimensional situation is different from the one-dimensional one), and for computational purposes (they provide testbeds for numerical approaches).

The case of a laminated material corresponds to the equation

$$-\operatorname{div}\left(\begin{pmatrix} a(\frac{x_1}{\varepsilon}) & 0 \\ 0 & a(\frac{x_1}{\varepsilon}) \end{pmatrix} \nabla u^\varepsilon(x_1,x_2)\right) = f, \tag{2.21}$$

which also reads

$$-\operatorname{div}\left(a(\frac{x_1}{\varepsilon})\big(\frac{\partial}{\partial x_1}u^\varepsilon(x_1,x_2)e_1 + \frac{\partial}{\partial x_2}u^\varepsilon(x_1,x_2)e_2\big)\right) = f. \tag{2.22}$$

We have denoted by (e_1, e_2) the canonical basis vectors in the two dimensional plane. The equation is considered on the square $Q = [0,1]^2$ and supplied with homogeneous Dirichlet boundary conditions. The function a is 1-periodic, and satisfies (2.10). It only depends on the first coordinate x_1 of $x = (x_1, x_2)$, thus the terminology "laminated". A prototypical example is

$$a(x_1) = \begin{cases} \alpha & \text{when} \quad 0 \le x_1 \le 1/2 \\ \beta & \text{when} \quad 1/2 < x_1 \le 1 \end{cases} \tag{2.23}$$

which corresponds in (2.21) to a model of a two-fold material consisting in lamellas, arranged along the direction x_1 of respective coefficients α and β, each lamella having thickness $\varepsilon/2$ (See Figure 1).

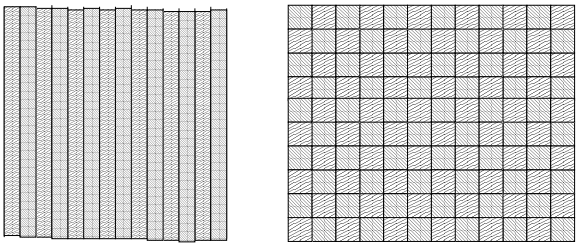

Figure 1: Left: Laminated material, the structure is invariant along direction x_2 and ε-periodic along direction x_1. Right: Two-dimensional checkerboard: although the amount of each "phase" is similar to that for the laminated material, the homogenized equation is drastically different.

The homogenized problem obtained from (2.21) is defined in the following:

Proposition 3. *As ε vanishes, the solution u^ε to (2.21) converges to the solution $u^\star$ to*

$$-\operatorname{div}\left(\begin{pmatrix} \dfrac{1}{< a^{-1} >} & 0 \\ 0 & < a > \end{pmatrix} \nabla u^\star\right) = f \tag{2.24}$$

that is

$$-\operatorname{div}\left(\frac{1}{< a^{-1} >}\frac{\partial}{\partial x_1}u^\star(x_1,x_2)e_1 + < a > \frac{\partial}{\partial x_2}u^\star(x_1,x_2)e_2\right) = f.$$

The result of the above Proposition is intuitively clear. In the direction x_1, the material behaves similarly to the one dimensional material studied in the previous section, while in the direction x_2, the material has no small scale oscillation and therefore responds as the classical algebraic average $< a >$ of its constitutive components.

Our second explicit example is a checkerboard material. We consider a function $a(x_1, x_2)$ periodic of the unit square Q, and piecewise constant, with values α and β both positive. See Figure 1. We then consider $A^\varepsilon = a(\frac{x_1}{\varepsilon}, \frac{x_2}{\varepsilon})\, Id$ and the solution u^ε in $H^1_0(Q)$ to

$$-\operatorname{div} A^\varepsilon \nabla u^\varepsilon = f, \tag{2.25}$$

that is,

$$-\operatorname{div}\left(\begin{pmatrix} a(\dfrac{x_1}{\varepsilon}, \dfrac{x_2}{\varepsilon}) & 0 \\ 0 & a(\dfrac{x_1}{\varepsilon}, \dfrac{x_2}{\varepsilon}) \end{pmatrix} \nabla u^\varepsilon(x_1,x_2)\right) = f$$

or

$$-\operatorname{div}\left(a(\frac{x_1}{\varepsilon}, \frac{x_2}{\varepsilon})\left(\frac{\partial}{\partial x_1}u^\varepsilon(x_1,x_2)e_1 + \frac{\partial}{\partial x_2}u^\varepsilon(x_1,x_2)e_2\right)\right) = f.$$

Then, we have

Proposition 4. *The solution u^ε to (2.25) converges to $u^\star \in H^1_0(\mathcal{D})$ solution to*

$$-\text{div}\, A^\star \nabla u^\star = f, \tag{2.26}$$

where

$$A^\star = \sqrt{\alpha\beta}\ Id. \tag{2.27}$$

For both the proofs of Propositions 3 and 4, we refer to the bibliography. The proofs are not difficult (especially the former) and are entirely based upon explicit analytical manipulations.

The comparison of the above two examples shows that, as announced, the main feature of dimension two is the onset of geometry. It is clear that the homogenized matrix obtained in the limit of vanishing ε is sensitive to the geometry of the combination of the two materials.

Two-scale expansion

Our two examples above are the only examples known to date for which an explicit expression of the homogenized matrix can be analytically obtained. All other cases require a different, non analytical approach.

From a theoretical result, Proposition 5, which will be given below, the existence of the homogenized matrix is ensured, but no information is given on its explicit expression. We present in this section an approach, called *two scale expansion*, which gives such an explicit expression. For now, the approach is formal. An outline of its mathematical foundation will be given a rigorous sense in Section 2.4 below.

We begin by *postulating* that the solution u^ε to (2.1) writes as the following expansion in powers of ε:

$$u^\varepsilon(x) = u_0(x, \frac{x}{\varepsilon}) + \varepsilon u_1(x, \frac{x}{\varepsilon}) + \varepsilon^2 u_2(x, \frac{x}{\varepsilon}) + ..., \tag{2.28}$$

where, at each order k, the function u_k is assumed to depend on two arguments: a macroscopic variable x and a microscopic variable $\dfrac{x}{\varepsilon}$. The dependence upon this latter variable is assumed periodic, that is

$$y \longrightarrow u_k(x, y) \text{ is periodic with periodic cell } Q = [0, 1]^d. \tag{2.29}$$

The form of the functions u_k appearing in the expansion is not (yet) made precise but a good prototypical form to think of to fix the ideas is the product of a "slowly" varying function in x by a "rapidly" varying function in $\frac{x}{\varepsilon}$. The approach now consists in inserting expansion (2.28) in (2.1) and equating powers in ε. The calculation is tedious but not difficult. All that needs to be borne in mind is the derivation rule:

$$\nabla \left(v(x, \frac{x}{\varepsilon})\right) = (\nabla_x v)(x,y) + \frac{1}{\varepsilon}(\nabla_y v)(x,y), \quad \text{where } y = \frac{x}{\varepsilon}, \tag{2.30}$$

where we denote by ∇_x and ∇_y the partial derivatives in x and y respectively. Of course, each one is a d-tuple of partial derivatives $(\frac{\partial}{\partial x_1}, ..., \frac{\partial}{\partial x_d})$.

We obtain an infinite hierarchy of equations (one for each order in ε):

$$\begin{aligned}
&-\mathrm{div}\,(A(y)\cdot\nabla u^\varepsilon) \\
&= -\frac{1}{\varepsilon^2}\mathrm{div}_y(A(y)\cdot\nabla_y u_0(x,y)) \\
&-\frac{1}{\varepsilon}\Big[\mathrm{div}_x(A(y)\cdot\nabla_y u_0(x,y)) + \mathrm{div}_y(A(y)\cdot\nabla_x u_0(x,y)) \\
&\qquad\qquad +\mathrm{div}_y(A(y)\cdot\nabla_y u_1(x,y))\Big] \\
&-\Big[\mathrm{div}_x(A(y)\cdot\nabla_x u_0(x,y)) + \mathrm{div}_y(A(y)\cdot\nabla_x u_1(x,y)) \\
&\qquad\qquad +\mathrm{div}_x(A(y)\cdot\nabla_y u_1(x,y)) + \mathrm{div}_y(A(y)\cdot\nabla_y u_2(x,y))\Big] \\
&\qquad\qquad +O(\varepsilon).
\end{aligned} \tag{2.31}$$

The nullity of the coefficient of $\frac{1}{\varepsilon^2}$ writes

$$\mathrm{div}_y(A(y)\cdot\nabla_y u_0(x,y)) = 0, \tag{2.32}$$

which yields

$$\nabla_y u_0(x,y) = 0. \tag{2.33}$$

Indeed:

$$\begin{aligned}
c\int_Q \left|\nabla_y u_0(x,y)\right|^2 &\leq \int_Q (A(y)\nabla_y u_0(x,y), \nabla_y u_0(x,y))\, dy \\
&\qquad \text{by coercivity of } A \\
&= -\int_Q \mathrm{div}_y(A(y)\cdot\nabla_y u_0(x,y))\, u_0(x,y)\, dy \\
&\quad +\int_{\partial Q} (A(y)\cdot\nabla_y u_0(x,y))\cdot n\ u_0(x,y),
\end{aligned}$$

where the first term vanishes because of (2.32) and the second term vanishes by periodicity of $u_0(x,y)$ with respect to y. We have denoted by n the unit outward normal on ∂Q. The condition (2.33) means that u_0 only depends on the macroscopic variable:

$$u_0 = u_0(x). \tag{2.34}$$

The term in $\dfrac{1}{\varepsilon}$ next gives:

$$-\mathrm{div}_y(A(y)\cdot(\nabla_x u_0(x) + \nabla_y u_1(x,y))) = 0.$$

The equation satisfied by u_1 therefore reads

$$\left\{ \begin{array}{rll} -\mathrm{div}_y(A(y)\cdot(\nabla_x u_0(x) + \nabla_y u_1(x,y))) & = 0, & \text{in } Q, \\ u_1 & & \text{periodic.} \end{array} \right. \tag{2.35}$$

Momentarily admitting that u_0 is known, and noticing the linearity of the equation, the solution to (2.35) may be explicitly written as

$$u_1(x,y) = \sum_{i=1}^{d} \frac{\partial u_0}{\partial x_i}(x) w_i(y), \tag{2.36}$$

where the functions w_i are the solutions to the following problems (called *cell-problems* or *corrector problems* in this setting):

$$\left\{ \begin{array}{rll} -\mathrm{div}_y(A(y)\cdot(e_i + \nabla_y w_i(y))) & = 0, & \text{in } Q, \\ w_i & & \text{periodic,} \end{array} \right. \tag{2.37}$$

where e_i, $i = 1, \ldots d$ denotes the i-th unitary vector of the canonical basis of $\mathbb{R}^d$. The functions w_i are only unique up to the addition of a constant, but it is easy to see in the argument that follows that, at least in this simple periodic setting and for the purpose of determining the dominant order in expansion (2.28), the value of the constant does not matter.

An important methodological remark is in order. Equation (2.35) that defines u_1 and will eventually (anticipating on the sequel) allow to express the homogenized matrix $A^\star$ is seen as an equation in the variable y, varying in the unit cell Q. In fact, in the early stages of our calculations, the variable y was not independent from the macroscopic variable x (we used to have $y = \dfrac{x}{\varepsilon}$). Here we in fact

(i) decouple y from x

(ii) deliberately make a confusion between $\frac{1}{\varepsilon}\mathcal{D}$ and $\mathbb{R}^d$, so that (2.35) is in fact posed on the entire space (consistent with the fact that, seen from the microscopic scale, $\mathcal{D}$ is an infinite domain)

(iii) and eventually use periodicity to set equation (2.35) only on Q.

None of these manipulations is clear. But this turns out to be the right perspective for this periodic setting, as the *proof* of the validity of the expansion will show. Other settings than this periodic linear setting can lead to significant related difficulties (see for instance the random setting in Section 4).

We finally identify u_0. To this end we return to (2.31) and look to the zero order term: in order for (2.1) to be satisfied, we need that:

$$\begin{aligned} -\mathrm{div}_y(A(y)\cdot(\nabla_x u_1(x,y)+\nabla_y u_2(x,y))) = \\ \mathrm{div}_x(A(y)\cdot(\nabla_y u_1(x,y)+\nabla_x u_0(x)))+f, \end{aligned} \tag{2.38}$$

along with periodic boundary conditions for u_2 on the boundary of Q.

A necessary (and actually sufficient) condition for the existence of a periodic function u_2 such that (2.38) holds is that the integral of the left hand side over the periodic cell vanishes. Indeed, if g is a periodic, vector-valued function,

$$\int_Q \mathrm{div}\, g(y)\, dy = \int_{\partial Q} g(y)\cdot n = 0.$$

The integral of the right-hand side of (2.38) therefore also vanishes, which yields

$$-\mathrm{div}_x\Big(\int_Q A(y)\cdot(\nabla_y u_1(x,y)+\nabla_x u_0(x))\, dy\Big) = f(x).$$

Inserting the value (2.36) of u_1 in terms of the functions w_i, we obtain

$$-\mathrm{div}_x\Big(\int_Q A(y)\cdot\sum_{j=1}^{d}\frac{\partial u_0}{\partial x_j}(x)(\nabla_y w_j(y)+e_j)\, dy\Big) = f(x). \tag{2.39}$$

Now

$$\begin{aligned}
&\int_Q A(y)\cdot\sum_{j=1}^{d}\frac{\partial u_0}{\partial x_j}(x)(\nabla_y w_j(y)+e_j)\,dy\\
&\quad=\int_Q A(y)\cdot\sum_{j=1}^{d}(\nabla u_0(x))_j(\nabla_y w_j(y)+e_j)\,dy\\
&\quad=\sum_{j=1}^{d}(\nabla u_0(x))_j\left(\int_Q A(y)\cdot(\nabla_y w_j(y)+e_j)\,dy\right)\\
&\quad=\sum_{i=1}^{d}\left(\sum_{j=1}^{d}\sum_{k=1}^{d}\int_Q A_{ik}(y)(\nabla_y w_j(y)+e_j)_k\,dy\,(\nabla u_0(x))_j\right)e_i\\
&\quad=\sum_{i=1}^{d}\left(\sum_{j=1}^{d}A^\star_{ij}(\nabla u_0(x))_j\right)e_i\\
&\quad=A^\star\cdot\nabla u_0(x)
\end{aligned}$$

where the entries of the matrix $A^\star$ read, for $i,j=1...N$,

$$A^\star_{ij}=\int_Q\left(A(y)\left(\nabla_y w_j(y)+e_j\right),e_i\right)dy. \tag{2.40}$$

An equivalent expression (using integration by parts) is

$$A^\star_{ij}=\int_Q\left(A(y)(e_i+\nabla_y w_i),(e_j+\nabla_y w_j)\right)dy. \tag{2.41}$$

Equation (2.39) now writes as the following *homogenized problem*

$$\left\{\begin{array}{rcl}-\mathrm{div}\,(A^\star\cdot\nabla u_0) &=& f,\quad \text{in}\,\mathcal{D},\\ u_0 &=& 0,\quad \text{on}\,\partial\mathcal{D}.\end{array}\right. \tag{2.42}$$

Determining the homogenized behaviour (behaviour for small ε) of the solution u^ε to (2.1) therefore requires a two step procedure

(i) solving for w_i solution to (2.37) for each direction i and computing the entries of $A^\star$ using (2.41),

(ii) solving for u_0 (also, for evident reasons, denoted by $u^\star$) solution to (2.42).

Computationally, we avoid solving one equation with a prohibitively fine mesh, and we prefer solving the N periodic problems (2.37) on the 'microscopic' unit cell, plus problem

(2.42) at scale 1 (therefore not needing any more a fine mesh, since ε is absent from the equation). Doing so, we find an *approximation* to u_ε solution to (2.1) at a certain order of accuracy in ε, as will be formalized below.

Remark 3. *Note that the approach is all the more efficient if we have to solve* (2.1) *for* many *right hand sides* f *(since problems* (2.37*) are independent of* f *and can be solved once and for all). The gain is also all the more important as* ε *is small.*

Proof of the correctness of the expansion

The calculations of the previous section are purely formal. They can be justified in many ways. We outline here two possible proofs, based on different arguments, that show that u^ε converges to u_0 solution to (2.42), in a sense made precise below. Much more can be found in the vast literature on the subject. We will primarily argue on the so-called *energy method* of Murat and Tartar. Then we shall mention the *two-scale convergence* approach by (independently) Nguetseng and Allaire.

The energy method. The *energy method*, more appropriately called the *method of oscillating test functions*, is due to Murat and Tartar [143, 171]. It is based on the principle of *compensated compactness*. We briefly sketch their proof. We do this in the periodic setting, but it should be borne in mind that the approach is not restricted to periodic setting and has been designed for more general settings. First, remark that the solution u^ε to (2.1) is bounded in H^1, and thus converges, up to an extraction, weakly in H^1. Similarly, $A(x/\varepsilon)\nabla u^\varepsilon$ converges weakly in L^2:

$$\nabla u^\varepsilon \rightharpoonup \nabla u_0 \text{ in } L^2, \tag{2.43}$$

$$A_{per}\left(\frac{x}{\varepsilon}\right)\nabla u^\varepsilon \rightharpoonup r_0 \text{ in } L^2. \tag{2.44}$$

Then, the solution w_p (for $p = e_i$) to (2.37) satisfies

$$\nabla w_p\left(\frac{x}{\varepsilon}\right) \overset{\star}{\rightharpoonup} \langle \nabla w_p \rangle = 0, \tag{2.45}$$

(where $\langle\cdot\rangle$ denotes the average in the periodic setting), thus:

$$p + \nabla w_p\left(\frac{x}{\varepsilon}\right) \overset{\star}{\rightharpoonup} p \text{ in } L^\infty. \tag{2.46}$$

In addition, we define $A^\star$ using the following weak limit:

$$A^T_{per}\left(\frac{x}{\varepsilon}\right)\left(p+\nabla w_p\left(\frac{x}{\varepsilon}\right)\right) \overset{\star}{\rightharpoonup} (A^\star)^T p \text{ in } L^\infty. \tag{2.47}$$

Note that this is equivalent to (2.40) in the periodic setting, given Proposition 1. Using that (2.43) and (2.46) are curl-free, and that (2.44) and (2.47) are divergence-free, the compensated compactness principle [143, 171] (or, more precisely here, the celebrated *div-curl Lemma*) allows to pass to the limit in both sides of

$$\left[A^T_{per}\left(\frac{x}{\varepsilon}\right)\left(p+\nabla w_p\left(\frac{x}{\varepsilon}\right)\right)\right]^T \nabla u^\varepsilon = \left(p+\nabla w_p(\frac{x}{\varepsilon})\right)^T \left[A_{per}\left(\frac{x}{\varepsilon}\right)\nabla u^\varepsilon\right],$$

getting

$$\left[(A^\star)^T p\right]^T \nabla u_0 = p^T r_0, \tag{2.48}$$

where r_0 is the weak limit of $A_{per}\left(\frac{x}{\varepsilon}\right)\nabla u^\varepsilon$. Recall that the *div-curl Lemma* states that when two sequences of vector valued functions $\mathbf{f}^{\boldsymbol{\varepsilon}}$ and $\mathbf{g}^{\boldsymbol{\varepsilon}}$ weakly converge in $\left(L^2(\mathcal{D})\right)^d$, respectively to $\mathbf{f}$ and $\mathbf{g}$, and are such that $\operatorname{div}\mathbf{f}^{\boldsymbol{\varepsilon}}$ is compact in $H^{-1}(\mathcal{D})$ and $\operatorname{curl}\mathbf{g}^{\boldsymbol{\varepsilon}}$ is compact in $\left(H^{-1}(\mathcal{D})\right)^d$, then the sequence of scalar products $\mathbf{f}^\varepsilon\,.\,\mathbf{g}^\varepsilon$ converges, at least in the sense of distributions to the scalar product $\mathbf{f}\,.\,\mathbf{g}$. The result is not evident since the product of two weakly converging sequences is typically unknown. The argument above is a direct application of the lemma.

All this is valid for *any* $p \in \mathbb{R}^d$. Thus equation (2.48), along with $-\operatorname{div}(r_0) = f$, gives the homogenized equation satisfied by u_0 (and equivalently proves that u_0 solution to this equation is the limit, weak in H^1 and strong in L^2, of the sequence u^ε).

The main two ingredients have been

(i) the weak convergence of rescaled functions (for A_{per} and ∇w_p),

(ii) the well-posedness of the corrector problem,

along with the compensated compactness principle.

The two-scale convergence method. An alternative method was introduced first by NGuetseng [146], and further developed by Allaire [3]. In contrast to the above energy method, designed for a general purpose, it was originally introduced to deal with the

periodic setting. In this setting, the crucial tool (which in some sense plays the role of the compensated compactness principle in the preceding method) is that any bounded sequence u^ε in H^1 satisfies the following convergences (up to extraction of a subsequence):

$$u^\varepsilon \longrightarrow u_0 \text{ in } H^1,$$
$$\forall \xi \in L^2(\mathcal{D}, L^2_{\rm per}(Q)), \quad \int_{\mathcal{D}} \nabla u^\varepsilon \xi\left(x, \frac{x}{\varepsilon}\right) dx \longrightarrow \int_{\mathcal{D}} \int_Q (\nabla u_0(x) + \nabla_y u_1(x,y)) \xi(x,y) dy dx,$$

for some $u_1 \in L^2(\mathcal{D}, H^1_{\rm per}(Q))$. Using this result, the proof of homogenization goes as follows: we multiply the first line of (2.1) by $\varphi_0(x) + \varepsilon\varphi_1\left(x, \frac{x}{\varepsilon}\right)$, where $\varphi_0 \in H^1(\mathcal{D})$ and $\varphi_1 \in H^1(\mathcal{D}, H^1_{\rm per}(Q))$, and use $\xi(x,y) = A(y)(\nabla\varphi_0(x) + \nabla_y\varphi_1(x,y))$ in the above convergence. This implies

$$\int_{\mathcal{D}} \int_Q (\nabla u_0(x) + \nabla_y u_1(x,y))\, A(y)(\nabla\varphi_0(x) + \nabla_y\varphi_1(x,y)) dy dx = \int_{\mathcal{D}} f\varphi_0. \tag{2.49}$$

It follows

$$-\text{div}_{\,y}\left[A(y)(\nabla u_0(x) + \nabla_y u_1(x,y))dy\right] = 0,$$

in Q with periodic boundary condition. This implies that

$$u_1(x,y) = \sum_{i=1}^d \frac{\partial u_0}{\partial x_i}(x) w_i(x).$$

Inserting this equation into (2.49) gives the homogenized problem.

Again, we see that the convergence of rescaled functions plays a key role, together with the definition of the corrector problem (in fact implicitly contained in (2.49)).

As we pointed out above, the two-scale convergence method was at first designed to deal with the periodic setting. However, it was then developed further to deal with much more general cases (see [147, 148, 149, 150]), which provide a nice, although rather technical, framework for putting the above formal considerations into mathematical terms. It remains that it intrinsically exploits the fact that we have two different scales: a micro scale, which we denote by ε, and a macro scale, which we set equal to 1. This explains the words "two-scale" convergence. In some sense, what depends on the micro scale is set on some unit cell (which is the unit cell of the periodic lattice in the periodic case), giving an "explicit" corrector equation. We thus have in this case a more explicit way of computing homogenized coefficients than with the energy method.

2.5 Revisiting the one-dimensional setting

It is instructive to return to the one-dimensional setting (2.9) for which we know (by specific one dimensional arguments) that the homogenized problem reads as (2.11). We *know* there that the limit of u^ε is:

$$u^\star =< a^{-1} > \left(-x \int_0^x f(t)\,dt + \int_0^x tf(t)\,dt + x\Big(\int_0^1 f(t)\,dt - \int_0^1 tf(t)\,dt\Big)\right), \tag{2.50}$$

the first derivative of which reads:

$$(u^\star)' =< a^{-1} > \left(- \int_0^x f(t)\,dt + \Big(\int_0^1 f(t)\,dt - \int_0^1 tf(t)\,dt\Big)\right). \tag{2.51}$$

On the other hand, the two-scale expansion claims that the limit is solution to

$$\left\{ \begin{array}{rcl} -\dfrac{d}{dx}\,(a^\star \dfrac{d}{dx} u_0) & = & f, \quad \text{in } [0,1], \\ u_0 & = & 0, \quad \text{at } 0 \text{ and } 1, \end{array} \right.$$

where the homogenized coefficient $a^\star$ is expressed as (2.41):

$$a^\star = \int_0^1 a(y)(1+w'(y))^2\,dy, \tag{2.52}$$

with w solution to (2.37), that is

$$\left\{ \begin{array}{rl} -\dfrac{d}{dy}(a(y)(1+\dfrac{d}{dy}w(y))) & = 0, \quad \text{in } [0,1], \\ w \text{ 1-periodic.} & \end{array} \right.$$

It is straightforward to see that

$$w'(y) = -1 + \frac{1}{< a^{-1} >}\,\frac{1}{a(y)}\,, \tag{2.53}$$

and thus that (up to an additive constant)

$$w(y) = -y + \frac{1}{< a^{-1} >} \int_0^y a^{-1}. \tag{2.54}$$

Inserting (2.53) into (2.52), we find the explicit value

$$a^\star = \int_0^1 a(y)(1+w'(y))^2\,dy = \int_0^1 a(y)\,\frac{1}{< a^{-1} >^2}\,\frac{1}{a(y)^2}\,dy = \frac{1}{< a^{-1} >}$$

which agrees with the value determined in Section 2.2. The result obtained using the two-scale expansion therefore agrees with the explicit one-dimensional approach.

The one dimensional setting allows us to move on to another issue: how to obtain the *strong* limit of u^ε in H^1. Since all calculations are explicit in dimension one, we may in fact determine the exact solution u^ε. It can be shown that

$$u^\varepsilon(x) = -\left(c_\varepsilon + \int_0^x f(t)\,dt\right) \int_0^x \frac{1}{a}(\frac{t}{\varepsilon})\,dt \;+\; \int_0^x \Big(\int_0^t \frac{1}{a}(\frac{t'}{\varepsilon})\,dt'\Big)\, f(t)\,dt \tag{2.55}$$

with the constant

$$\begin{aligned} c_\varepsilon &= \frac{-\displaystyle\int_0^1 \frac{1}{a}(\frac{t}{\varepsilon})\,dt \int_0^1 f(t)\,dt \;+\; \int_0^1 \Big(\int_0^t \frac{1}{a}(\frac{t'}{\varepsilon})\,dt'\Big)\, f(t)\,dt}{\displaystyle\int_0^1 \frac{1}{a}(\frac{t}{\varepsilon})\,dt} \\ &= -\langle a(\frac{\cdot}{\varepsilon})^{-1}\rangle^{-1} \int_0^1 a(\frac{\cdot}{\varepsilon})^{-1} F, \end{aligned} \tag{2.56}$$

where we have denoted by $F(x) = \displaystyle\int_0^x f(t)dt$. We now consider:

$$\begin{aligned} (u^\varepsilon)' - (u_0)' &= \left(-\frac{1}{a}(\frac{x}{\varepsilon}) + < \frac{1}{a} >\right)\left(c_\varepsilon + \int_0^x f(t)\,dt\right) \\ &- < a^{-1} > \left(c_\varepsilon + \int_0^1 f(t)\,dt - \int_0^1 t f(t)\,dt\right). \end{aligned}$$

We easily note (using an argument similar to that used in the proof of Proposition 1) that

$$c_\varepsilon + \int_0^1 f(t)\,dt - \int_0^1 t f(t)\,dt = O(\varepsilon). \tag{2.57}$$

On the other hand, the first term of the right hand side only *weakly* converges to zero, again using Proposition 1. That convergence is (generically) never strong, and we deduce that $(u^\varepsilon)' - (u_0)'$ only *weakly* converges to zero in L^2.

To improve the approximation, we now form the difference

$$(u^\varepsilon(x))' - (u_0(x) + \varepsilon u_0'(x) w(\frac{x}{\varepsilon}))',$$

making use of the first two terms of the two scale expansion. After some simple computations, we obtain

$$\begin{aligned} (u^\varepsilon(x))' - \big(u_0(x) + \varepsilon u_0'(x) w(\frac{x}{\varepsilon})\big)' &= -\frac{1}{a}(\frac{x}{\varepsilon}) \left(c_\varepsilon + \int_0^1 f(t)\,dt - \int_0^1 t f(t)\,dt\right) \\ &+ \big(-x \;< a^{-1} > + \int_0^x a^{-1}(\frac{t}{\varepsilon})\,dt\big)\, f(x), \end{aligned} \tag{2.58}$$

where (2.57) and Proposition 1 now give a strong convergence of the right-hand side (in fact they show that (2.58) is a $O(\varepsilon)$ in $L^\infty([0,1])$). We therefore obtain

$$u^\varepsilon(x) - (u_0(x) + \varepsilon u_0'(x) w(\frac{x}{\varepsilon})) \text{ converges to 0 in } H^1(\mathcal{D}). \tag{2.59}$$

Note that this shows, in the one-dimensional setting (see Proposition 5 below for a general statement), that the first two terms of the two scale expansion allow for a strong convergence in H^1. This motivates the terminology *corrector problem* for (2.37): the function w (called the *corrector*) allows to *correct* the weak H^1 convergence of u^ε to u_0 and makes it strong. Note also that we do not claim (and it is indeed not correct, as a simple one-dimensional computation would easily show it) that the remainder in (2.59) is $o(\varepsilon)$. Note finally that $u_0(x) + \varepsilon u_0'(x) w(\frac{x}{\varepsilon})$ does *not* satisfy the homogeneous Dirichlet boundary condition satisfied by u^ε itself. The quality of the local convergence is thus expected to degrade when approaching the boundaries of the domain $\mathcal{D}$, and this is indeed the case.

2.6 Energy viewpoint

We briefly present in this section a different viewpoint on the problems considered. When the matrix A_{per} is symmetric, equation (2.1) may be seen as the Euler-Lagrange (or optimality) equation of the following mimization problem

$$\inf_{u \in H_0^1(\mathcal{D})} \frac{1}{2} \int_{\mathcal{D}} (\nabla u(x)\,,\, A_{per}(\frac{x}{\varepsilon})\, \nabla u(x))\, dx \,-\, \int_{\mathcal{D}} f(x) u(x)\, dx. \tag{2.60}$$

It is therefore natural to ask about a possible similar variational definition of the homogenized problem. It is indeed possible to first define the homogenized matrix $A^\star$ as

$$\forall z \in \mathbb{R}^d, \;\; z\, A^\star\, z = \inf_{\substack{\nabla u \text{ periodic} \\ \int_Q \nabla u = z}} \int_Q (\nabla u(y)\,,\, A_{per}(y)\, \nabla u(y))\, dy. \tag{2.61}$$

Proving that (2.60) agrees with our former definition of the homogenized matrix is easy (and left to the reader) in the one-dimensional setting. It is more intricate in higher dimensions. Next, the homogenized solution u_0 may be expressed as the minimizer to

$$\inf_{u \in H_0^1(\mathcal{D})} \frac{1}{2} \int_{\mathcal{D}} \left(\inf_{\substack{\nabla v \text{ periodic} \\ \int_Q \nabla v = \nabla u(x)}} \int_Q (\nabla v(y)\,,\, A(y)\, \nabla v(y))\, dy \right) dx \,-\, \int_{\mathcal{D}} f u\,. \tag{2.62}$$

2.7 An incursion into the general theory

The periodic setting we have considered so far is a simple setting. In fact, most results established above can be extended to a more general setting. It usually comes at the price of losing the "explicitness". The general result states:

Proposition 5. *Let $\mathcal{D}$ be a bounded domain in $\mathbb{R}^d$, and let A^ε be a sequence of invertible matrices with entries in $L^\infty(\mathbb{R}^d)$, satisfying $A^\varepsilon \geq c_1 Id$ and $(A^\varepsilon)^{-1} \geq c_2 Id$ (in the sense $\forall x \in \mathbb{R}^d$, $(A^\varepsilon x, x) \geq c_1 \|x\|^2$, and likewise for $(A^\varepsilon)^{-1}$) for two constants $c_i > 0$ independent from ε. Then, there exists a* homogenized *matrix $A^\star$ satisfying the same properties as A^ε and a subsequence $A^{\varepsilon'}$ of the original sequence A^ε so that, for all functions $f \in H^{-1}(\mathcal{D})$, the function u^ε solution in $H^1_0(\mathcal{D})$ to*

$$-\mathrm{div}\, A^\varepsilon \nabla u^\varepsilon = f \tag{2.63}$$

converges in the following sense

$$u^{\varepsilon'} \rightharpoonup u^\star\,,\ A^{\varepsilon'}\nabla u^{\varepsilon'} \rightharpoonup A^\star \nabla u^\star\,,\ A^{\varepsilon'}\nabla u^{\varepsilon'} \cdot \nabla u^{\varepsilon'} \rightharpoonup A^\star \nabla u^\star \cdot \nabla u^\star \tag{2.64}$$

respectively in weak-$H^1_0(\mathcal{D})$, weak-$L^2(\mathcal{D})$ and in the distribution sense. In addition,

$$\int_{\mathcal{D}} A^{\varepsilon'}\nabla u^{\varepsilon'} \cdot \nabla u^{\varepsilon'}\, dx \longrightarrow \int_{\mathcal{D}} A^\star \nabla u^\star \cdot \nabla u^\star\, dx, \tag{2.65}$$

where $u^\star \in H^1_0(\mathcal{D})$ solves

$$-\mathrm{div}\, A^\star \nabla u^\star = f. \tag{2.66}$$

This proposition is part of the *theory of H-convergence*, by F. Murat and L. Tartar in the 1970s, a theory that generalizes the *theory of G-convergence*, by S. Spagnolo, which was restricted to the case of *symmetric* operators.

The main two points of the result are

- that the matrix $A^\star$ and the subsequence ε' do *not* depend on the right-hand side f: in the terminology of Mechanics, an homogenized "material" exists, the same whatever the load;
- that the homogenized equation obtained is of the same form as the original equation (this is not evident, and many counter-examples exist for other settings, we refer to the bibliography).

In contrast, the major weakness of the result is that *no explicit* expression of $A^\star$ is provided. The periodic context was one possible context to obtain explicit expressions. The random ergodic context presented in Section 4 below is another one. In homogenization theory, there is always a balance between generality and explicitness!

The last couple of theoretical results we will mention deals with the term at next order:

Proposition 6 (Theorem of correctors). *Under the assumptions of Proposition* 5*, there exist* N *sequences of functions* $z_i^{\varepsilon'} \in H^1(\mathcal{D})$ *satisfying*

$$z_i^{\varepsilon'} \overset{\varepsilon'\longrightarrow 0}{\rightharpoonup} 0, \text{ weakly in } H^1(\mathcal{D}), \tag{2.67}$$

and

$$-\operatorname{div} A^{\varepsilon'}\left(e_i + \nabla z_i^{\varepsilon'}\right) \overset{\varepsilon'\longrightarrow 0}{\longrightarrow} -\operatorname{div} A^\star\, e_i, \text{ strongly in } H^{-1}(\mathcal{D}), \tag{2.68}$$

such that

$$\nabla u^{\varepsilon'} - \left(\mathrm{Id} + \nabla z^{\varepsilon'}\right) \nabla u^\star \overset{\varepsilon'\longrightarrow 0}{\longrightarrow} 0, \text{ strongly in } (L^1(\mathcal{D}))^d. \tag{2.69}$$

The functions z_i *are called the* correctors*, since they allow for a strong convergence of* $u^{\varepsilon'}$ *to* $u^\star$ *in (*2.69*).*

Corollary 7. *Under the assumptions and with the notation of Proposition* 5*, the homogenized matrix* $A^\star$ *reads*

$$A^\star = \lim_{\text{weak in } (L^2(\mathcal{D}))^{d\times d}} A^{\varepsilon'}\left(\mathrm{Id} + \nabla z^{\varepsilon'}\right). \tag{2.70}$$

It is easy to see, comparing with the periodic setting, how (2.68) and (2.70) respectively relate to our cell problems (2.37) and the average (2.40) (note that in the periodic case $-\operatorname{div} A^\star\, e_i = 0$ since $A^\star$ does not depend on x). Similarly, as is the case in the periodic setting presented above, correctors allow to "explicitly" express the homogenized matrix (although the explicitness is arguable!)

3 Numerical issues

Solving practically the homogenized problem in the periodic setting is rather straightforward. The corrector problem (2.2) is first solved as a variational problem posed on a

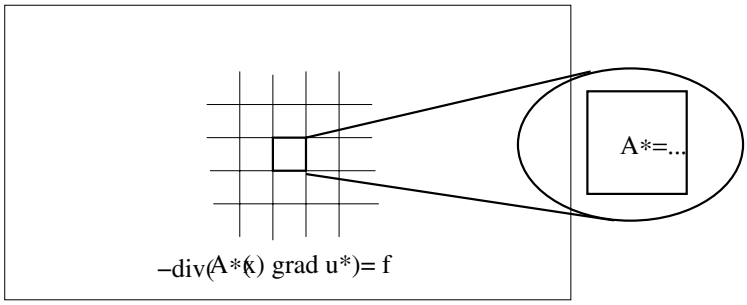

Figure 2: Schematic representation of periodic (and locally periodic) homogenization: The homogenized matrix, used in the equation replacing the original, highly oscillating equation, is constructed "cell by cell"

bounded domain with periodic boundary conditions. Next, the homogenized matrix $A^\star$ is constructed using (2.3), and the homogenized problem (2.4) is finally solved on a mesh of size $H \gg \varepsilon$.

An easy adaptation of the above strategy allows to address *locally periodic* problems, that is problems of the type (2.1) with a coefficient matrix $A_{per}(x, \frac{x}{\varepsilon})$ that is periodic on its second argument. Then, one corrector problem per macroscopic point x needs to be solved, and the homogenized matrix is in fact a x-dependent matrix $A^\star(x)$. The computational situation is schematized on Figure 2.

A new category of methods have appeared in the past few years. They provide an alternate approach to the above "direct" homogenization strategy. One motivation for their introduction is to obtain the solution to (2.1) for some parameter ε that is small, *without* using the asymptotics $\varepsilon \longrightarrow 0$. The hope is to better approximate the solution u^ε for ε that is not too small. Practice shows that this hope is generally achieved, although the regime where the approach is computationally efficient still corresponds to rather small values of ε.

We only outline here the bottom line for such methods, which carry several names. One instance is the *MultiScale finite Element Method* (MsFEM). We refer to [77] for a more exhaustive presentation of that approach, and only look here at a prototypical, academic example of the approach.

The idea to obtain an efficient numerical approach is to start from the following basic

observation. The difficulty of (2.1) and problems of the same type is that the computational approach needs to capture the small oscillations of the solution u^ε inherited from those of the coefficient matrix $A_{per}(\frac{\cdot}{\varepsilon})$. As earlier mentioned, a general purpose finite element basis set is only able to capture these oscillations if the meshsize is taken sufficiently small. An alternative approach is to use basis functions that are not generic, but are specifically designed for the problem at hand (somewhat in the spirit of *spectral methods* in other contexts of scientific computing). In order to build such basis functions, the idea is to consider the two-scale expansion introduced above:

$$u^\varepsilon(x) = u_0(x) + \varepsilon \sum_{i=1}^{d} \frac{\partial u_0}{\partial x_i}(x) w_i(\frac{x}{\varepsilon}).$$

This expression encodes the fact that the corrector functions, obtained solving the cell problems at the microscopic scale, contribute to the accuracy of the approximation of u^ε. Thus the idea is to solve boundary problems *reminiscent* of the cell problem, and then to use the solutions to these problems in the construction of the finite element basis. There are several variants of the idea, due to several authors.

Suppose for simplicity we work in dimension 2, and that the computational domain is meshed using squares and $Q1$ finite elements denoted by ψ_i. We may for instance determine the functions η_i^ε solution to

$$\left\{ \begin{array}{rcll} -\mathrm{div}\,(A(\frac{x}{\varepsilon}) \cdot \nabla(\eta_\varepsilon^i + \psi^i)) & = & 0, & \text{on a typical mesh cell,} \\ \eta_\varepsilon^i & = & 0, & \text{on the boundary,} \end{array} \right.$$

and next set $\varphi_\varepsilon^i = \eta_\varepsilon^i + \psi^i$, which solves

$$\left\{ \begin{array}{rcll} -\mathrm{div}\,(A(\frac{x}{\varepsilon}) \cdot \nabla\varphi_\varepsilon^i) & = & 0, & \text{on a typical mesh cell} \\ \varphi_\varepsilon^i(x_j) & = & \delta_{ij}, & \text{at the vertices } x_j \text{ of the cell} \\ \varphi_\varepsilon^i & & \text{is continuous} & \text{crossing edges.} \end{array} \right.$$

The functions φ_ε^i are then adopted as finite element basis set. Note that the small oscillations are *encoded* in the basis itself, and thus the finite element solution is likely to be of better quality, for a given meshsize h still large as compared to ε.

The above described approach has of course an applicability way beyond the periodic context.

4 Stochastic Homogenization

4.1 Basic mathematical setting and main result

The present section introduces the classical *stationary ergodic setting*. Throughout the section, $(\Omega, \mathcal{F}, \mathbb{P})$ denotes a probability space. For any random variable $X \in L^1(\Omega, d\mathbb{P})$, we denote by $\mathbb{E}(X) = \int_\Omega X(\omega) d\mathbb{P}(\omega)$ its expectation value. We fix $d \in \mathbb{N}^\star$, and assume that the group $(\mathbb{R}^d, +)$ acts on Ω. We denote by $(\tau_k)_{k\in\mathbb{R}^d}$ this action, and assume that it *preserves the measure* $\mathbb{P}$, i.e

$$\forall x \in \mathbb{R}^d, \quad \forall B \in \mathcal{F}, \quad \mathbb{P}(\tau_x B) = \mathbb{P}(B). \tag{4.1}$$

We assume that τ is *ergodic*, that is,

$$\forall B \in \mathcal{F}, \quad \big(\forall x \in \mathbb{R}^d, \quad \tau_x B = B\big) \Rightarrow (\mathbb{P}(B) = 0 \quad \text{or} \quad 1). \tag{4.2}$$

In addition, we define *stationarity*: any $F \in L^1_{\rm loc}\left(\mathbb{R}^d, L^1(\Omega)\right)$ is said to be *stationary* if

$$\text{for almost } y \in \mathbb{R}^d, \quad F(x+y,\omega) = F(x,\tau_y\omega) \text{ almost everywhere in } x, \text{ almost surely.} \tag{4.3}$$

The ergodic theorem [100, 165] can be stated as follows:

Theorem 8 (Ergodic theorem, [100, 165]). *Let $F \in L^\infty\left(\mathbb{R}^d, L^1(\Omega)\right)$ be a stationary random variable in the sense of (4.3). Then*

$$\frac{1}{B_R}\int_{B_R} F(x,\tau_y\omega)\, dy \underset{R\to\infty}{\longrightarrow} \mathbb{E}\left(F\right) \quad \text{in } L^\infty(\mathbb{R}^d), \text{ almost surely.} \tag{4.4}$$

This implies that

$$F\left(\frac{x}{\varepsilon}, \omega\right) \overset{\star}{\underset{\varepsilon\to 0}{\rightharpoonup}} \mathbb{E}\left(F\right) \quad \text{in } L^\infty(\mathbb{R}^d), \text{ almost surely.} \tag{4.5}$$

It is useful to intuitively define stationarity and ergodicity in terms of material modeling. Pick two points x and $y \neq x$ at the microscale in the material. The particular local environment seen from x (that is, the microstructure present at x) is generically different from what is seen from y (that is, the microstructure present at y). However, the *average* local environment in x is identical to that in y (considering the various realizations of the

random material). In mathematical terms, the *law* of microstructures (here modelled by the coefficient matrix A in (4.6) below) is the same at all points. This is *stationarity*. It is then possible to construct a group action τ that satisfies the above properties. On the other hand, *ergodicity* means that considering all the points in the material amounts to fixing a point x in this material and considering all the possible microstructures present there.

Note that periodicity is indeed a particular case of the stationary ergodic setting. It is obtained taking Ω the N dimensional torus $\mathbb{R}^d/\mathbb{Z}^d$, letting $\mathbb{P}$ be the Lebesgue measure on Ω, and defining the group action τ by $\tau_x y = x + y \bmod \mathbb{Z}^d$, for all $(x, y) \in \mathbb{R}^d \times \Omega$. It is easily checked that τ_x preserves the Lebesgue measure and that it is ergodic. But of course, the stochastic ergodic setting is *much broader* than the periodic setting.

We now fix $\mathcal{D}$ an open, smooth and bounded subset of $\mathbb{R}^d$, and A a square matrix of size d, which is assumed stationary ergodic in the sense defined above, and which is assumed to enjoy the classical assumptions of uniform ellipticity and boundedness. Then we consider the boundary value problem

$$\begin{cases} -\mathrm{div}\left(A\left(\frac{x}{\varepsilon}, \omega\right) \nabla u^\varepsilon\right) = f \quad \text{in} \quad \mathcal{D}, \\ u^\varepsilon = 0 \quad \text{on} \quad \partial\mathcal{D}. \end{cases} \tag{4.6}$$

Standard results of stochastic homogenization [28, 99] apply and allow to find the homogenized problem for problem (4.6). These results generalize the periodic results recalled in Section 2. The solution u^ε to (4.6) converges (weakly in H^1 and almost surely in ω) to the solution to the *deterministic* problem (2.4) where the homogenized matrix is now defined as:

$$[A^\star]_{ij} = \mathbb{E}\left(\left(e_i + \nabla w_{e_i}(y, \cdot)\right)^T A\left(y, \cdot\right) e_j\right), \tag{4.7}$$

where for any $p \in \mathbb{R}^d$, w_p is the solution (unique up to the addition of a (random) constant) in $\left\{w \in L^2_{\mathrm{loc}}(\mathbb{R}^d, L^2(\Omega)), \quad \nabla w \in L^2_{\mathrm{unif}}(\mathbb{R}^d, L^2(\Omega))\right\}$ to

$$\begin{cases} -\mathrm{div}\left[A\left(y, \omega\right)\left(p + \nabla w_p(y, \omega)\right)\right] = 0, \quad \text{a.s. on} \quad \mathbb{R}^d \\ \nabla w_p \quad \text{is stationary in the sense of (4.3)}, \\ \mathbb{E}\left(\nabla w_p(y, \cdot)\right) = 0. \end{cases} \tag{4.8}$$

We have used above the notation $L^2_{\rm unif}$ for the *uniform* L^2 space, that is the space of functions for which, say, the L^2 norm on a ball of unit size is bounded above independently from the center of the ball. The fact that, in this simple linear elliptic case, the corrector allows to obtain a strong convergence in H^1 of u^ε is for example proved in [154].

A striking difference between the stochastic setting and the periodic setting can be observed comparing (2.2) and (4.8). In the periodic case, the corrector problem is posed on a bounded domain (namely, the periodic cell Q). In sharp contrast, the corrector problem (4.8) of the random case is posed on the whole space $\mathbb{R}^d$, and cannot be reduced to a problem posed on a bounded domain (it will be, but only for computational purposes). The reason is, condition $\mathbb{E}\left(\nabla w_p(y,\cdot)\right) = 0$ in (4.8) is a *global* condition. It indeed equivalently reads, because of the ergodic Theorem, a.s. $-\lim_{R\longrightarrow+\infty} \dfrac{1}{|B_R|}\displaystyle\int_{B_R} \nabla w_p(y,\cdot)\,dy = 0$ for any sequence of balls B_R of radii R. The fact that the random corrector problem is posed on the entire space has far reaching consequences both for the theory and for numerical practice. For the theory, we observe we have to work in a non compact context. This is one of the, if not *the*, major difficulty of stochastic homogenization. It is not too critical here, because we are in a simple (meaning: strongly elliptic, in divergence form) and linear setting, but for, say, nonlinear situations, this non compactness causes huge difficulties, and leaves unsolved many problems. For the numerical approximation, this is also a serious issue. Truncations of problem (4.8) have to be considered, and the actual homogenized coefficients are only deterministic, and correct in the asymptotic regime.

Remark 4. *It is well known that, even in the periodic setting, some of the difficulties we mention for the random setting already arise when the operator is, for instance, nonlinear. Then determining the periodic homogenized problem cannot always be reduced to a simple computation on one single periodic cell of the problem. Likewise, proving that a corrector function exists, and that it indeed allows to have a strong convergence in H^1 can be difficult, or open.*

4.2 Simple analysis

Like in the periodic case, it is instructive to consider the "zero-dimensional" and one-dimensional settings. We will in particular be able to highlight some important differences

between the periodic and the stationary ergodic settings. Since we have laid some groundwork in the periodic case, we will be able to argue more rapidly here. Besides the little technicalities mentioned here, the reader should bear in mind that the outcome of the discussion is that the random context for homogenization is incredibly much richer than the periodic context. To some extent, random homogenization is *generic*.

Deleting all the differential operators in (4.6) and considering a one-dimensional context immediately shows that the question is, again, to identify the weak limit, as ε vanishes, of the sequence $b(\frac{x}{\varepsilon},\omega)$ for b a stationary ergodic function. It is exactly the purpose of the ergodic theorem, Theorem 8, to determine this limit, namely $\mathbb{E}(b)$, and states that it is an almost sure limit.

Moving on to the one-dimensional setting

$$\left\{\begin{array}{rcl} -\dfrac{d}{dx}(a(\dfrac{x}{\varepsilon},\omega)\dfrac{d}{dx}u^\varepsilon) &=& f, \quad \text{in }]0,1[\\ u^\varepsilon(0)=u^\varepsilon(1) &=& 0, \end{array}\right. \tag{4.9}$$

we of course can exploit our computations in the periodic case. On the one hand, we know the exact solution u^ε by (2.55)-(2.56), the formula holding almost surely in ω. On the other hand, we may solve the corrector problem

$$\left\{\begin{array}{l} -\dfrac{d}{dy}(a(y,\omega)(1+w'(y))) \quad = 0, \quad \text{in } [0,1], \\ w' \text{ stationary}\,, \mathbb{E}(w')=0, \end{array}\right.$$

and find, similarly to in (2.54) that, up to an additive constant,

$$w(y,\omega) = -y + \left(\mathbb{E}(a^{-1})\right)^{-1} \int_0^y a^{-1}(x,\omega)\,dx. \tag{4.10}$$

This of course yields the value $a^\star = \left(\mathbb{E}(a^{-1})\right)^{-1}$ for the homogenized coefficient appearing in the homogenized equation, that is the one-dimensional version of (2.4). Like in the periodic case, it is elementary to prove that u^ε converges to the solution $u^\star$ of the latter equation. The convergence holds weakly in H^1 and, this time, almost surely in ω. Including the corrector allows for a (almost sure in ω) strong convergence in H^1 of $u^\varepsilon(x,\omega) - \left(u^\star(x) + \varepsilon\,(u^\star)'(x)\,w(\frac{x}{\varepsilon},\omega)\right)$ to zero.

Although the ergodic stochastic setting shares many properties of the periodic setting, even the consideration of the one-dimensional simple situation allows to exhibit some striking differences. We have already seen that a major difference is that the corrector problem is posed on the entire space, and not on a bounded domain (the periodic cell). We now mention two additional differences: the nature of the corrector and the rate of convergence.

It is easily remarked on (4.10) that the corrector w is *not* a stationary function. Only its first derivative $w'(x) = -1 + \left(\mathbb{E}(a^{-1})\right)^{-1} a^{-1}(x,\omega)$ is. In the periodic setting, both functions were periodic. This is in fact related to the following phenomenon, not restricted to the one-dimensional setting. If ∇w is a periodic function that has zero mean, then w is a periodic function (and, of course, conversely). In contrast, if ∇w is a stationary function with $\mathbb{E}(\nabla w) = 0$, then we do not necessarily have w stationary, but we only can claim that w is *sublinear at infinity*, that is $(1+|x|)^{-1} w$ converges to zero as $|x| \longrightarrow +\infty$, almost surely in ω (this is a consequence of the ergodic theorem, and can be easily verified *e.g.* using (4.10)). Even though the homogenized matrix involves only the gradient of the corrector, and not the corrector itself, this observation complicates the situation.

In the one-dimensional setting, we have the explicit expressions of u^ε and $u^\star$, which are of course valid, only changing the notation (the average is replaced by the expectation value, and the dependence upon ω is possibly indicated), both in the periodic and the stationary ergodic settings. We are thus able to explicitly express the rate of the convergence of the latter to the former. We have seen in (2.58) the explicit expression of the difference $(u^\varepsilon)' - \left(u^\star + \varepsilon\,(u^\star)'\,w(\frac{\cdot}{\varepsilon})\right)'$. We easily deduce that

$$u'_\varepsilon(x) - (1 + w'\left(\frac{x}{\varepsilon}\right))\,(u^\star)'(x) = -\,(c_\varepsilon - c_\star)\; a(\frac{x}{\varepsilon})^{-1}, \tag{4.11}$$

where c_ε is, we recall, defined in (2.56) and where we denote by $c_\star = -\displaystyle\int_0^1 F$. It follows that, in the periodic case, the difference scales, in L^∞-norm (and thus L^2-norm), as ε:

$$(u^\varepsilon)' - \left(1 + w'(\frac{\cdot}{\varepsilon})\right)\,(u^\star)' = O(\varepsilon) \tag{4.12}$$

The exact same expression for the stochastic case shows, using a central limit theorem, that

$$\sqrt{\varepsilon}^{-1}\left[(u^\varepsilon)' - \left(1 + w'(\frac{\cdot}{\varepsilon})\right)\,(u^\star)'\right] \text{ converges in law to a Gaussian.} \tag{4.13}$$

We note that for a central limit theorem to hold, we need to assume more than ergodicity. The appropriate setting is to assume *mixing*, which is a condition ensuring that correlations become sufficiently small at large distance. In this simplified presentation, let us only mention that if the coefficients $a(x,\omega)$ and $a(y,\omega)$ are independent for $x \neq y$, then mixing holds. Likewise, considering now the functions and not their first derivatives, two straightforward calculations show that in the periodic setting

$$u^\varepsilon - u^\star = O_{L^2}(\varepsilon), \tag{4.14}$$

while in the stochastic setting

$$\sqrt{\varepsilon}^{-1}\,[u^\varepsilon - u^\star] \text{ converges in law.} \tag{4.15}$$

A striking contrast between the periodic and the stationary setting is the above different scalings. For the reader not familiar with probability theory, let us briefly mention why the above convergences can well be expected to hold at the indicated rates. We only argue, for brevity, on (4.12) and (4.13). The other two convergences (4.14)-(4.15) proceed from the same type of arguments. In (4.11), we observe that

$$c_\varepsilon - c_\star = \int_0^1 F - \frac{\int_0^1 a(\frac{\cdot}{\varepsilon})^{-1} F}{\int_0^1 a(\frac{\cdot}{\varepsilon})^{-1}},$$

and hence deduce that the rate of convergence is directly inherited from the rate at which, in the "zero-dimensional" setting, the oscillating function $b(\frac{\cdot}{\varepsilon}) = a(\frac{\cdot}{\varepsilon})^{-1}$ converges to its weak limit (its average). It is easily seen on the proof of Proposition 1 (using (2.7)) that, if b is periodic, then $b(\frac{\cdot}{\varepsilon}) - < b >$ weakly converges to zero at the rate $O(\varepsilon)$. On the other hand, this is the purpose of the central limit theorem (here for ergodic stationary functions) to state that, when b is stationary ergodic $\sqrt{\varepsilon}^{-1}\left[b(\frac{\cdot}{\varepsilon},\omega) - \mathbb{E}(b)\right]$ converges in law to a Gaussian. This, along with elementary manipulations, entirely explains the different rates of convergence in (4.12) through (4.15).

4.3 Two-dimensional and more general settings

In dimensions higher than one, as we now know well because of our experience with the periodic setting, we do not have any explicit expression for the functions manipulated.

Like in the periodic case, there are almost no exactly solvable model either. The only explicit case the author is aware of is the so-called *random checkerboard*, which is the exact analogous setting to the periodic case mentioned in Section 2.4: the (scalar) coefficient is defined on the unit cube and randomly takes values α and β, each with probability $1/2$, on each of the quarters of the cube. Within the cube and from one cube to any other, all random variables are independent. Then the homogenized matrix is again given by (2.27).

In full generality, delicate arguments have to be conducted. It is out of the question to prove in these introductory lecture notes that the main results announced in Section 4.1 indeed hold. In order to give a flavour of the difficulties specific to the stationary ergodic setting, we will only outline here the proof of the existence of the corrector, that is the solution to (4.8). As mentioned above, the difficulty is that we need to work on the entire space $\mathbb{R}^d$. The idea is to lift all the differential calculus on the abstract probability space, and use the variational theory (Lax-Milgram Lemma and related notions). But, even then, a remaining difficulty is the absence of any Poincaré inequality. To circumvent the difficulty, we need to *approximate* problem (4.8). This is typically performed introducing the following auxiliary problem: *search for a stationary function* $w_{p,\eta}$ *such that*

$$-\mathrm{div}\left[A\left(y,\omega\right)\left(p+\nabla w_{p,\eta}(y,\omega)\right)\right]+\eta\, w_{p,\eta}=0, \tag{4.16}$$

on the whole space, for $\eta>0$ *supposedly small.* On the abstract probability space, the problem reads

$$-\mathrm{DIV}\left[A\left(p+\mathrm{GRAD}\quad W_{p,\eta}\right)\right]+\eta\, W_{p,\eta}=0, \tag{4.17}$$

where we have used obvious notation for the divergence and gradient differential operators on the abstract space, and for $W_{p,\eta}$ corresponding to $w_{p,\eta}$ in the sense $w_{p,\eta}(x,\omega)=W_{p,\eta}(\tau_x\omega)$. A simple application of the Lax-Milgram lemma proves the existence and uniqueness of the stationary function $W_{p,\eta}$. It is then easy to show, by coercivity, L^2 bounds on $\mathrm{GRAD}\, W_{p,\eta}$ and $\sqrt{\eta}W_{p,\eta}$respectively, that are independent of η. It follows that, up to an extraction, we have weak convergence of the sequence of gradients $\nabla w_{p,\eta}(y,\omega)$, to some stationary function that is necessarily a gradient $\nabla w_p(y,\omega)$. Equation (4.8) is easily obtained passing to the limit of vanishing η (note that the approximating term $\eta\, w_{p,\eta}$ vanishes because it reads $\sqrt{\eta}$ times a bounded function). The condition $\mathbb{E}\left(\nabla w_p(y,\cdot)\right)=0$ is also

easily obtained from the weak convergence and $\mathbb{E}\left(\nabla w_{p,\eta}(y,\cdot)\right) = 0$ which holds because $w_{p,\eta}$ is itself stationary. We note that, as expected, no stationarity is known on w_p itself.

For all other questions related to the linear elliptic problems in divergence form under consideration here, we refer the reader to the bibliography. The general message is, somewhat vaguely stated, that, apart from the already mentioned differences, all what is true in the periodic setting is still true here. Problems that are not variational, or that are nonlinear, or both, are orders of magnitude more difficult. For the nonlinear non variational case, anything can happen! And it is certainly not the appropriate place here, in this introductory exposition, to present the many difficulties or open problems present in that context. The take-away message is, again loosely stated, that each single issue that is simple in the linear case (existence, uniqueness of the corrector, etc) can become extremely difficult, can admit a different answer, or is still an unsolved question. We refer to [132, 166] for examples of important contributions on various issues. Note that several of these difficulties are already present in the periodic, nonlinear nonvariational case. They are just even more difficult in the random context.

4.4 Numerical approaches

The first practical task is the computation of the homogenized matrix $A^\star$. The matrix $A^\star$ is approximated by the matrix

$$\left[A_N^\star\right]_{ij}(\omega) = \frac{1}{|Q_N|}\int_{Q_N}\left(e_i + \nabla w_{e_i}^N(y,\omega)\right)^T A(y,\omega)\left(e_j + \nabla w_{e_j}^N(y,\omega)\right)\,dy \tag{4.18}$$

which is in turn obtained by solving the corrector problem (4.8) on a *truncated* domain, say the cube $Q_N \subset \mathbb{R}^d$ of size $(2N+1)^d$ centered at the origin:

$$\begin{cases} -\mathrm{div}\,\left(A(\cdot,\omega)\left(p + \nabla w_p^N(\cdot,\omega)\right)\right) = 0 \quad \text{on} \quad \mathbb{R}^d, \\ w_p^N(\cdot,\omega) \text{ is } Q_N\text{-periodic.} \end{cases} \tag{4.19}$$

Although $A^\star$ itself is a deterministic object, its practical approximation $A_N^\star$ is random. It is only in the limit of infinitely large domains Q_N that the deterministic value is attained. On the theoretical level, new questions arise on the convergence of approximations, precisely related to the random nature of the objects. On a practical level, questions about how to improve rates of convergence and also how to control *variance* issues enter the picture.

There are several (in fact not that many) existing works in the literature that examine some aspects of numerical stochastic homogenization. We wish to cite:

- the original contribution [179] by Yurinski, where the convergence of some truncated approximation of $A^\star$ is established, along with an estimate of the rate of convergence (in short, problem (4.8) is regularized and then $A^\star$ is approximated on a bounded domain),
- a similar study [47] by Bourgeat and Piatnitsky for a specific approximation more relevant to actual numerical practice (in short, both problem (4.8) and the expectation (4.7) (seen as a normalized integral over the whole space) are truncated as in (4.18)–(4.19)),
- the work [144] by Naddaf and Spencer on a discrete ("lattice-type") approximation of the differential operator present in the original problem (4.6),
- and the enterprise by Gloria and Otto (see [89] for homogenization problems set on random lattices and publications announced in preparation for some problems for differential operators) to establish sharp estimates of the convergence of the numerical approximation in terms of size of the truncation domain and other discretization parameters.

Besides the above works, where the focus is on convergence and rates of convergence, practical issues are to improve prefactors in convergences and also reduce variance in the empirical means everywhere used to approximate expectation values. We refer the reader to the recent works [32, 33, 64, 65] for more details on these issues.

Alternative approaches are, like in the periodic context outlined in Section 3, based upon determining suitable finite element basis sets, well adapted to the problem at hand. The approach is still in its infancy for the random context, and we believe many interesting tracks for future research are possible, see [176].

Finally, we wish to mention a series of works the purpose of which is to approximate random homogenization problems that only contain "a small amount" of randomness (in a sense made precise) using a set of deterministic problems, see the overview article [116] and the contributions [9, 10, 11, 63].

In any event, it has to be clear in the reader's mind that numerical random homogenization is still a field very much unexplored, as compared to other computational problems in partial differential equations. As a sign of this, we mention that, in the engineering or mechanics communities, random homogenization is often performed with very crude approaches: most often only *bounds* on the homogenized coefficients are utilized, and when a numerical approximation of the coefficient itself is seeked, the computational approach is still very much *ad hoc*. Many textbooks are available that describe the practical approaches used in the applied disciplines. Obviously, there is still much room for improvement.

5 Atomistic to Continuum modelling

This section presents a rather recent, multiscale strategy used for modelling solid materials. The strategy consists in concurrently coupling two different levels of description of matter: atomistic modelling on the one hand, continuum mechanics on the other hand.

As announced in the introduction, this section is adapted from [42]. The review article [122] has also been useful.

5.1 Continuum elasticity theory

To begin with, we need to lay some groundwork, recalling some basic elements on the standard mechanical description of a solid material subjected to forces. For simplicity and brevity, the setting is *static*. We refer *e.g.* to the monograph [57] for a complete mathematically oriented presentation including time-dependent situations.

We denote by $\mathcal{D}$ the reference domain that the material occupies at rest, by φ the deformation it is subjected to, i.e. the map from $\mathcal{D}$ to $\mathbb{R}^3$ that gives the current position of the material. We also denote by $u(x) = \varphi(x) - x$ the displacement, and by $\nabla\varphi : \mathcal{D} \longrightarrow \mathcal{M}_3$ the gradient of deformation, where $\mathcal{M}_3$ denotes the space of square matrices of size 3×3. The general equations that describe the equilibrium of our sample material, when subjected to body forces f and boundary forces g, read

$$-\text{div } T = f \quad \text{in } \mathcal{D}, \tag{5.1}$$

with the boundary condition $T \cdot n = g$ on $\partial\mathcal{D}$. Here, T denotes the stress tensor (more

precisely the first Piola-Kirchhoff stress tensor), and n is the unitary outward normal vector on $\partial\mathcal{D}$.

In order to close the equation (5.1), a relation is needed between the stress tensor T and the kinematic description of the material, provided by the fields φ, u or F. In contrast to equations (5.1) which are general, the relation linking T to, say, φ, depends on the material considered. In such a relation is indeed encoded the physical and mechanical nature of the material. Formally, such a closure relation reads

$$T = T(x, \varphi(x), ...), \tag{5.2}$$

and is called a *constitutive relation*, or a *law of behavior*. Equation (5.2) is symbolic: derivatives of φ may also be inserted, as well as other points than x (or, in a time-dependent setting, times anterior to the time t at which the stress tensor is evaluated). The relation may be a differential equation, a partial differential equation, an integral equation, etc.

A commonly used framework is

$$T(\varphi) = \frac{\partial W}{\partial(\nabla\varphi)}(\nabla\varphi), \tag{5.3}$$

where W is the *density of mechanical energy*. Actually, owing to the fact that the laws of mechanics are invariant under rigid rotations, the function W may only depend on $\nabla\varphi$ via $\nabla\varphi^T\nabla\varphi$. Along with (5.3), equation (5.1) is then recognized as the Euler-Lagrange equation for the minimization of a problem of the form

$$\inf_{\varphi\in\mathcal{A}} \int_{\mathcal{D}} W(\nabla\varphi(x))\,dx - \int_{\mathcal{D}} f\,\varphi - \int_{\partial\mathcal{D}} g\,\varphi, \tag{5.4}$$

where $\mathcal{A}$ is the set of all *admissible* deformations φ. We omit several technical (and actually also fundamental) issues in this expository presentation, see for example the works [21, 57]. The most famous example of density W is provided by *linearized elasticity*. Then, W is the simple quadratic form

$$W = \frac{1}{2}\boldsymbol{\varepsilon} : A : \boldsymbol{\varepsilon} \quad \text{where} \quad \boldsymbol{\varepsilon} = \frac{1}{2}(\nabla u + \nabla u^T) \quad \text{and} \quad u(x) = \varphi(x) - x. \tag{5.5}$$

This model has the advantage that the Euler-Lagrange equations of the variational problem (5.4), with W given by (5.5), are *linear*. Note however that this density W is *not* invariant under rigid rotations.

For a given material, the derivation of the constitutive law (5.2) is a central theoretical question, and a challenging practical issue. Then, the resolution of (5.1), or the minimization of (5.4), is the purpose of the numerical simulations performed. Despite all these efforts, and all the expertise accumulated, the strategy for the derivation of a constitutive law for a solid material is delicate and challenging. Therefore, it is useful to develop an alternative strategy: multiscale modelling.

We emphasize that bypassing the macroscopic constitutive law is one of the major purpose of multiscale modelling in materials science. In principle, the constitutive law is expected to encode the physical nature of the material, so that the phenomena taking place at all the scales finer than the macroscopic ones are accounted for. A multiscale model is also aimed at encoding such a relation, but, in contrast, without translating it into an *explicit* mathematical relation. The physical nature of the material is inserted via an explicit microscopic description, which is in turn coupled with the usual macroscopic description of the material. Loosely speaking, the derivation of the constitutive law is *implicitly* performed by the simulation itself. The amount of physical intuition needed is expected to be smaller, the computational effort will compensate for it. Likewise, it is hoped that less modeling assumptions will be needed: ideally, a universal microscopic model is inserted in the universal macroscopic description. In doing so, the sources for inaccuracies are easier to identify, and the assessment of the quality of the result is simpler.

5.2 Bottom line for Atomistic-to-continuum modelling for crystals

When a model for the density of mechanical energy (5.3) for a given solid material is unknown, one has to return to the microscopic scale, and use appropriate atomistic models. The task is then to deduce from the atomistic scale an appropriate density of mechanical energy, that is, a specific form for a constitutive law (5.2).

To this end, we proceed as follows: we give ourselves a microscopic description of the sample, next we fix the deformation φ that is imposed to the material at the macroscopic level and directly apply it to the atomic sites at the microscopic level, and we search for the macroscopic limit of the energy obtained.

We expect to derive an explicit form for the macroscopic mechanical energy of the sample deformed by φ, thus a link between the density of mechanical energy W, and the

energy model used at the microscopic level.

For simplicity, we consider an elementary two-body interaction potential at the atomic scale, and place the atoms on a particularly simple geometrical arrangement. At the microscopic scale, the material occupies the domain $\mathcal{D}$, and we assume its substructure is the truncation $\mathcal{D} \cap \mathcal{L}$ of a periodic lattice $\mathcal{L}$. Every pair of sites $(\overline{x_i}, \overline{x_j})$ in $\mathcal{D} \cap \mathcal{L}$ interacts with a pair potential $V(\overline{x_i} - \overline{x_j})$. We assume the periodic lattice has a cubic unit cell, and that the atomic site stands at the center of this cell. The length of the cell is denoted by ε, and vanishes in the macroscopic limit. The potential V, taken radially symmetric, is assumed to be smooth, and have compact support. No body force, nor boundary force, is applied to the material. The deformation we apply to the sample is assumed to be smooth. All these assumptions aim at avoiding unnecessary technicalities.

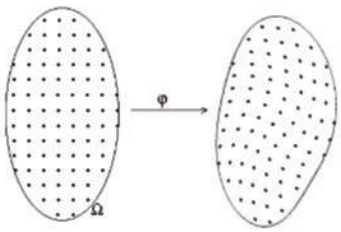

Figure 3: Deformation φ of a crystalline material.

We now apply the deformation φ (see Figure 3). The microscopic energy formally reads:

$$\frac{1}{2}\frac{1}{N^3} \sum_{\overline{x_i} \in (N\mathcal{D}) \cap \mathbb{Z}^3} \sum_{\overline{x_j} \neq \overline{x_i} \in (N\mathcal{D}) \cap \mathbb{Z}^3} V\left(\frac{\varphi\left(\frac{\overline{x_i}}{N}\right) - \varphi\left(\frac{\overline{x_j}}{N}\right)}{\frac{1}{N}} \right). \tag{5.6}$$

In fact the above sum is truncated over a finite domain, containing $N = \varepsilon^{-1}$ sites per dimension. It is normalized by the total number of particles (since the energy is an extensive quantity). Note also that we need to rescale all distances by a factor $\frac{1}{N} = \varepsilon$, so that the equilibrium length (i.e., say, the length r that minimizes the function $r \longrightarrow V(r)$) is also of order ε for consistency. The purpose is now to identify the limit of (5.6) when $N \longrightarrow \infty$. This means that we both let the truncated lattice go to the whole infinite lattice at the microscopic scale, and let the lattice size vanishes, so as to pass to the macroscopic limit.

In this simple case, the analysis is obvious. As φ is smooth, we write its Taylor expansion at the first order and neglect the terms of higher order:

$$\frac{\varphi\left(\frac{\overline{x_i}}{N}\right) - \varphi\left(\frac{\overline{x_j}}{N}\right)}{\frac{1}{N}} = N\left(\varphi\left(\frac{\overline{x_i}}{N}\right) - \varphi\left(\frac{\overline{x_j}}{N}\right)\right) \approx \nabla\varphi\left(\frac{\overline{x_j}}{N}\right)\cdot(\overline{x_i} - \overline{x_j}). \tag{5.7}$$

We insert this in the potential V, and in turn search for the first order. Arguing formally, omitting some technicalities in particular related to boundary terms that can be easily handled, and using the periodicity of the lattice, we see that the limit formally reads

$$\lim_{N\longrightarrow+\infty} \frac{1}{N^3}\frac{1}{2} \sum_{\overline{x_j}\in(N\mathcal{D})\cap\mathbb{Z}^3} \sum_{\overline{x_k}\neq 0\in\mathbb{Z}^3} V\left(\nabla\varphi\left(\frac{\overline{x_j}}{N}\right)\cdot\overline{x_k}\right). \tag{5.8}$$

Denoting by

$$\Psi(x) = \frac{1}{2}\sum_{\overline{x_k}\neq 0\in\mathbb{Z}^3} V\left(\nabla\varphi(x)\cdot\overline{x_k}\right), \tag{5.9}$$

we observe that (5.8) is a Riemann sum in Ψ, and converges as $N\longrightarrow+\infty$ to

$$\frac{1}{|\mathcal{D}|}\int_{\mathcal{D}}\Psi(x)\,dx = \frac{1}{2|\mathcal{D}|}\int_{\mathcal{D}}\sum_{\overline{x_k}\neq 0\in\mathbb{Z}^3} V\big(\nabla\varphi(x)\cdot\overline{x_k}\big)\,dx \tag{5.10}$$

where $|\mathcal{D}|$ is the volume of the domain $\mathcal{D}$. At the macroscopic level, the (non-dimensional) density of mechanical energy therefore reads

$$W(\nabla\varphi(x)) = \frac{1}{2}\sum_{\overline{x_k}\neq 0\in\mathbb{Z}^3} V\big(\nabla\varphi(x)\cdot\overline{x_k}\big). \tag{5.11}$$

We observe that this energy is indeed the energy of the original periodic lattice *deformed by the linear map* $\nabla\varphi(x)$ at the macroscopic point x. A simple example is the case of the quadratic potential $V\propto|r-r_{eq}|^2$ where r_{eq} denotes some equilibrium interatomic distance. It is easily seen, at least formally and in dimension one (and if particles stay ordered), that the above derivation then yields the linearized elasticity model (5.5) as a limit in (5.11). For the simple case treated here (periodic lattice, pair-potential interaction), this derivation of a macroscopic density of energy has been known for long. The work [39] presents a rigorous and systematic study of such a question. In fact, the approach may be generalized to a large variety of settings: various energy models and various geometries at the microscopic scale, various shapes of materials, etc. See for instance, in the bibliography, the related works [54, 38, 39, 40].

In full generality, the expressions obtained are all of the form

$$W(\nabla\varphi(x)) = \text{Energy of the microstructure at macro point } x \text{ deformed by } \nabla\varphi(x). \quad (5.12)$$

The multiscale nature of the model is obvious on that expression.

It is illustrative to mention a slight extension of the simple case presented above. We consider, instead of a periodic lattice of atomic sites as the microscopic model for the crystalline structure, a random perturbation of this arrangement. More explicitly, we assume that, before rescaling, the atomic sites now stand at points $\overline{x_i}(\omega) = i + X_i(\omega)$, where i is the three-dimensional integer index that also denotes an arbitrary point of $\mathbb{Z}^3$, and where $X_i(\omega)$ is a set of ergodic stationary random variables. Then, arguing as above, but this time additionally using the ergodic theorem, the density of mechanical energy obtained in the macroscopic limit reads

$$W(\nabla\varphi(x)) = \mathbb{E}\left[\frac{1}{2}\sum_{k\neq 0\in\mathbb{Z}^3} V\left(\nabla\varphi(x)\cdot(k+X_k(\omega)-X_0(\omega))\right)\right], \quad (5.13)$$

instead of (5.11). We refer to the original paper [39] for the details of the derivation.

The above derivation of the continuum mechanics energy (5.10) from the atomistic energy (5.6) is based on a smoothness assumption on the deformation φ. In many situations of interest (for instance when dislocations appear, as in the nanoindentation simulation shown in Figure 4), such an assumption does not hold in the whole domain, and one cannot use a model based on (5.10). Using an atomistic model in the whole domain is not possible either, due to its prohibitive computational cost. We now describe a coupling method, whose motivation is based on the observation that, actually, the deformation that we are after is not smooth in *only a small part* of the solid. So, a natural idea is to try to take advantage of both models, the continuum mechanics one and the atomistic one, and to couple them, in a domain decomposition spirit. The description below is a toy-version of the QuasiContinuum Method (QCM), as presented in its initial version [169, 168] by E.B. Tadmor, M. Ortiz and R. Phillips. The method has been next amended, and we will describe a more mature formulation in Section 5.3.

The microscopic energy of a given deformation φ is (5.6), that we recast as

$$E_{\text{micro}}(\varphi) = \frac{1}{N^3}\sum_{\overline{x_i}\in(N\mathcal{D})\cap\mathbb{Z}^3} E_i(\varphi),$$

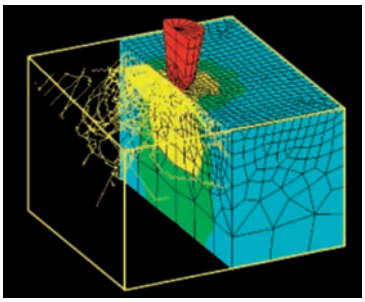

Figure 4: A typical numerical simulation coupling discrete and continuum mechanics, in a cube of size 2 μm (Courtesy M. Fivel, INPG; see also the work [81] by M.C. Fivel, C.F. Robertson, G.R. Canova and L. Boulanger).

where

$$E_i(\varphi) = \frac{1}{2} \sum_{\overline{x_j} \in (N\mathcal{D}) \cap \mathbb{Z}^3,\ \overline{x_j} \neq \overline{x_i}} V\left(\frac{\varphi\left(\frac{\overline{x_i}}{N}\right) - \varphi\left(\frac{\overline{x_j}}{N}\right)}{\frac{1}{N}} \right) \tag{5.14}$$

denotes the energy of atom i.

We now split the computational domain $\mathcal{D}$ into two non-overlapping subdomains,

$$\mathcal{D} = \mathcal{D}_{\rm reg} \cup \mathcal{D}_{\rm sing}, \tag{5.15}$$

where $\mathcal{D}_{\rm reg}$ is a domain where the deformation is expected to be smooth (see Figure 5). Consequently, in $\mathcal{D}_{\rm reg}$, we can approximate the atomistic energy by a continuum mechanics expression, in the spirit of (5.10)-(5.11). In $\mathcal{D}_{\rm sing}$, we cannot make this approximation, and we keep the original atomistic model. For a given deformation φ, we hence write

$$\begin{aligned} E_{\rm micro}(\varphi) &= \frac{1}{N^3} \sum_{\overline{x_i} \in (N\mathcal{D}_{\rm reg}) \cap \mathbb{Z}^3} E_i(\varphi) + \frac{1}{N^3} \sum_{\overline{x_i} \in (N\mathcal{D}_{\rm sing}) \cap \mathbb{Z}^3} E_i(\varphi) \\ &\approx \frac{1}{N^3} \sum_{\overline{x_i} \in (N\mathcal{D}_{\rm reg}) \cap \mathbb{Z}^3} \Psi\left(\frac{\overline{x_i}}{N}\right) + \frac{1}{N^3} \sum_{\overline{x_i} \in (N\mathcal{D}_{\rm sing}) \cap \mathbb{Z}^3} E_i(\varphi), \end{aligned} \tag{5.16}$$

where Ψ is defined by (5.9). The expression (5.16) is next approximated by

$$\begin{aligned} E_c(\varphi, \mathcal{D}_{\rm reg}) &= \frac{1}{|\mathcal{D}|} \int_{\mathcal{D}_{\rm reg}} \Psi(x)\, dx + \frac{1}{N^3} \sum_{\overline{x_i} \in (N\mathcal{D}_{\rm sing}) \cap \mathbb{Z}^3} E_i(\varphi) \\ &= \frac{1}{|\mathcal{D}|} \int_{\mathcal{D}_{\rm reg}} W(\nabla\varphi(x))\, dx + \frac{1}{N^3} \sum_{\overline{x_i} \in (N\mathcal{D}_{\rm sing}) \cap \mathbb{Z}^3} E_i(\varphi). \end{aligned} \tag{5.17}$$

Recall that $\Psi(x) = W(\nabla\varphi(x))$ is the energy of an atom in an infinite system deformed by the linear map $\nabla\varphi(x)$. The domain $\mathcal{D}_{\rm reg}$ is hence often called the *local zone*, since only the knowledge of the deformation φ in a neighborhood of x is needed to compute the energy of an atom located at x. The situation is completely different in $\mathcal{D}_{\rm sing}$. We make the standard assumption that, beyond a cut-off radius r_c, the potential V vanishes. Hence only the atoms inside the ball of center x and of radius r_c interact with an atom located at $x \in \mathcal{D}$. In view of (5.17) and (5.14), we see that the energy of an atom of $\mathcal{D}_{\rm sing}$, located at $\varphi(\overline{x_i}/N)$, depends on the positions of *all* the atoms in a ball of radius r_c around $\varphi(\overline{x_i}/N)$, and not only on the values of φ in a neighborhood of $\varphi(\overline{x_i}/N)$.

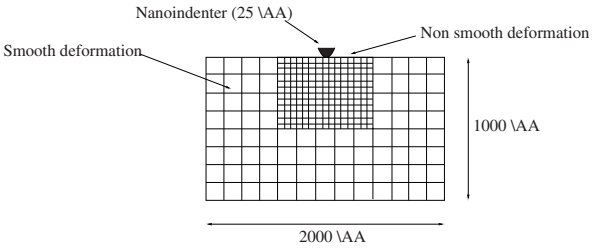

Figure 5: Schematic representation of a nanoindentation experiment: close to the stiff indenter, one expects a non-smooth deformation of the soft material, hence the need of a fine model. Further away, the deformation is smooth, and a macroscopic model, discretized on a coarse mesh (here quadrangles), provides a good enough accuracy.

In practice, a finite element method is employed in $\mathcal{D}_{\rm reg}$ to approximate the deformation φ. The first term of (5.17) is computed by a numerical quadrature, involving a few quadrature points in each finite element. In the case of a piecewise linear approximation, the degrees of freedom are the values of φ on the vertices of the mesh in $\mathcal{D}_{\rm reg}$, and the positions $\varphi\left(\overline{x_j}/N\right)$ of the atoms belonging to $\mathcal{D}_{\rm sing}$ (that is, those such that $\overline{x_j} \in (N\mathcal{D}_{\rm sing}) \cap \mathbb{Z}^3$).

An equilibrium configuration $\varphi_{\rm eq}$ is defined as the global minimizer of an approximation of (5.17), along the above lines (note that some methods alternatively focus on *local* minimizers, rather than global ones, or on critical points of the energy). This configuration only makes sense if it is smooth in $\mathcal{D}_{\rm reg}$. Indeed, in that region, we replaced the original atomistic energy by a continuum mechanics energy, which is possible only under some regularity assumptions on the deformation. If, according to a certain criterion which is

part of the multiscale method, the deformation $\varphi_{\rm eq}$ is considered not smooth in a subdomain $\mathcal{D}_{\rm irreg}$ of $\mathcal{D}_{\rm reg}$, then the partition (5.15) is updated accordingly, and a new partition $\mathcal{D} = \mathcal{D}_{\rm reg}^{\rm new} \cup \mathcal{D}_{\rm sing}^{\rm new}$, defined by

$$\mathcal{D}_{\rm reg}^{\rm new} = \mathcal{D}_{\rm reg} \setminus \mathcal{D}_{\rm irreg}, \quad \mathcal{D}_{\rm sing}^{\rm new} = \mathcal{D}_{\rm sing} \cup \mathcal{D}_{\rm irreg},$$

is considered: the domain $\mathcal{D}_{\rm irreg}$, which was described at the continuum scale, is now described at the atomistic scale. A coupled energy of type (5.17), based on this new partition, is considered. This yields the following iterative procedure. Start with a given partition of $\mathcal{D}$, and then iterate over the steps:

- on the basis of the current partition, define the coupled energy (5.17);
- solve the variational problem associated with that energy (we denote $\varphi_{\rm eq}$ its global minimizer);
- update the partition on the basis of $\varphi_{\rm eq}$, along the lines of the above discussion.

We now assess the computational gain. Evaluating the energy of atom i is more expensive when using the nonlocal model (5.14) than when using the local model (5.9). Indeed, in the local formulation (5.9), it is easy to compute the position of all the atoms in the ball of cutoff radius around atom i. On the other hand, computing the energy of atom i according to the nonlocal expression (5.14) requires to know all the positions $\varphi\left(\overline{x_j}/N\right)$ of the atoms j in the cutoff radius ball centered around atom i. This is a computationally demanding task, since one first has to determine in which finite element each of these atoms j is. Besides, in practice, finite elements of the subdomain $\mathcal{D}_{\rm reg}$ contain a very large number of atoms n_e. As a consequence, computing the contribution of the local zone $\mathcal{D}_{\rm reg}$ to the total energy is much cheaper with the coarse-grained model than with the reference model. Indeed, in the coarse-grained model, this contribution, which is exactly the first term of (5.17), can be computed by evaluating the energy of an *extremely small* number of atoms (those at the quadrature points, where Ψ needs to be evaluated). In constrast, in the reference model, one has to compute the energy of a *large* number n_e of atoms. So the computational gain comes from a two-fold argument: in $\mathcal{D}_{\rm reg}$, the energy of much fewer atoms needs to be evaluated, and each of these evaluations is cheaper, since a local model is used rather than a nonlocal one.

5.3 Numerical approaches

The method analyzed in Section 5.2 is a model example for more advanced methods, such as the QuasiContinuum Method (QCM). In its initial version [168, 169], the approach first considers the continuum scale, with a standard continuum mechanics model, discretized by a finite element method. The multiscale feature of the method appears when the elastic energy of an element is computed. Depending on some criteria, some elements are declared to be too heterogeneously strained for a macroscopic description to be valid. They are considered henceforth as a set of discrete particles. The associated energy is then computed according to an underlying atomistic model. Otherwise, for an element that is smoothly deformed, the standard original continuum mechanics model is used to compute the energy.

In the second, posterior, version of the method [163] that we describe below, the opposite viewpoint is adopted. The starting point is a multibody atomistic energy,

$$E_{\rm micro}(\varphi) = \sum_{i=1}^{N} E_i(\varphi), \tag{5.18}$$

sum of the energies $E_i(\varphi)$ of each individual atom i when the current configuration of the atomistic system is defined by φ. We define the equilibrium configuration as the solution to

$$\inf \left\{ E_{\rm micro}(\varphi);\ \varphi \in \mathcal{A} \right\}, \tag{5.19}$$

with

$$\mathcal{A} = \left\{ \varphi \in \mathbb{R}^{dN},\ \varphi \text{ satisfies some boundary conditions} \right\},$$

where d is the space dimension. In practice, the system under consideration is composed of an extremely large number N of atoms. Hence, the evaluation of (5.18), for a given φ, is already a challenging task. Furthermore, the variational problem (5.19) is set in a high-dimensional space.

To drastically diminish the number N of degrees of freedom, N_r atoms are selected, with $N_r \ll N$. They are called the representative atoms, abbreviated *repatoms*. Let i_α, $1 \leq \alpha \leq N_r$, denote their indices. Their current positions $\{\varphi^{i_\alpha}\}_{\alpha=1}^{N_r}$ are the only remaining degrees of freedom of the reduced system. The positions of the $N - N_r$ non-representative

atoms are obtained by interpolation. The idea of interpolation is related to the Cauchy-Born rule, see the work [86]. More precisely, a mesh is built upon the repatoms in the reference configuration. Let φ_0^i be the reference position of atom i, and $S_\alpha(x)$ be the piecewise affine function associated with the node α (for simplicity, we henceforth consider a P1 finite element method). In a one-dimensional setting, we thus have

$$S_\alpha(x) = \begin{cases} \dfrac{x - \varphi_0^{i_{\alpha-1}}}{\varphi_0^{i_\alpha} - \varphi_0^{i_{\alpha-1}}} & \text{if } \ \varphi_0^{i_{\alpha-1}} \le x \le \varphi_0^{i_\alpha}, \\ \dfrac{x - \varphi_0^{i_{\alpha+1}}}{\varphi_0^{i_\alpha} - \varphi_0^{i_{\alpha+1}}} & \text{if } \ \varphi_0^{i_\alpha} \le x \le \varphi_0^{i_{\alpha+1}}, \\ 0 & \text{otherwise.} \end{cases}$$

The position of any atom i in the deformed configuration is obtained from the current positions of the repatoms using the interpolation formula

$$\varphi^i = \sum_{\alpha=1}^{N_r} S_\alpha(\varphi_0^i)\ \varphi^{i_\alpha}. \tag{5.20}$$

Otherwise stated, a Galerkin approximation

$$\inf \{E_{\text{micro}}(\varphi);\ \varphi \in \mathcal{A} \text{ and satisfies (5.20)}\} \tag{5.21}$$

of (5.19) is performed.

We now turn to the practical evaluation of the energy (5.18), and explain how to handle the large number of terms it involves. Assume that the energy of atom i reads

$$E_i(\varphi) = \frac{1}{2} \sum_{j \neq i, \|\varphi^j - \varphi^i\| \le r^{\text{cut}}} V(\varphi^j - \varphi^i) \tag{5.22}$$

for some interaction potential V with some cutoff radius r^{cut}, and assume that the reference configuration is a periodic lattice. Consider an atom i that only interacts with the atoms j of the same finite element. The key point is to observe that its energy $E_i(\varphi)$ actually does not depend on i. Indeed, when atoms i and j belong to the same finite element, on which S_α is an affine function, we infer from (5.20) that

$$\varphi^j - \varphi^i = \sum_{\alpha=1}^{N_r} \left(g_\alpha^\ell \cdot (\varphi_0^j - \varphi_0^i)\right)\ \varphi^{i_\alpha},$$

where g_α^ℓ is the gradient of S_α in the finite element ℓ, which is a *constant* vector. Hence, $\varphi^j - \varphi^i$ is a function of $\varphi_0^j - \varphi_0^i$, parameterized by the finite element ℓ and the current positions $\{\varphi^{i_\alpha}\}_{\alpha=1}^{N_r}$ of the repatoms:

$$\varphi^j - \varphi^i = \mathcal{F}\left(\varphi_0^j - \varphi_0^i; \ell, \{\varphi^{i_\alpha}\}_{\alpha=1}^{N_r}\right).$$

Inserting the above relation in (5.22), we observe that $E_i(\varphi)$ is a sum of terms that only depend on $\varphi_0^j - \varphi_0^i$, that we write

$$E_i(\varphi) = \frac{1}{2}\sum_{j\neq i} \widetilde{\mathcal{F}}\left(\varphi_0^j - \varphi_0^i; \ell, \{\varphi^{i_\alpha}\}_{\alpha=1}^{N_r}\right).$$

The reference configuration being a perfect lattice, we obtain that the above sum actually does not depend on i.

Hence, all atoms i in a finite element ℓ that only interact with atoms j in the same finite element share the same energy, which we may thus denote by E_ℓ, and which only depends on the current positions of the repatoms (actually, only on those related to the vertices of the finite element): $E_i(\varphi) = E_\ell\left(\{\varphi^{i_\alpha}\}_{\alpha=1}^{N_r}\right)$. By choice, the exact same expression $E_\ell\left(\{\varphi^{i_\alpha}\}_{\alpha=1}^{N_r}\right)$ is taken as an approximation of the energy of atoms that interact with atoms belonging to different finite elements. We hence approximate the energy (5.18) using

$$\widetilde{E}_{\rm micro}(\varphi) = \sum_\ell n_\ell E_\ell\left(\{\varphi^{i_\alpha}\}_{\alpha=1}^{N_r}\right), \tag{5.23}$$

where n_ℓ is the number of atoms included in the finite element ℓ. Note that there are much fewer terms in the sum (5.23) than in the sum (5.18). We next approximate (5.21) by the problem

$$\inf\left\{\widetilde{E}_{\rm micro}(\varphi);\ \varphi \in \mathcal{A} \text{ and satisfies (5.20)}\right\}, \tag{5.24}$$

which can be solved in practice, since it is posed on a space of moderate dimension (there are $dN_r \ll dN$ degrees of freedom), and it involves energies $\widetilde{E}_{\rm micro}(\varphi)$ that can be computed practically.

So, in its second version, the QuasiContinuum method somewhat consists in an efficient quadrature rule to compute (5.18). This second formulation leads to similar equations as the first version, presented in Section 5.2, in the case of a discretization using Lagrangian P1 finite elements. Indeed, in that case, the degrees of freedom in both the first and second

versions are the current positions of the atoms at the mesh vertices. In addition, using the fact that $\nabla\varphi$ is constant over each triangle T_ℓ, the first term of (5.17) reads

$$\frac{1}{|\mathcal{D}|}\int_{\mathcal{D}_{\rm reg}} W(\nabla\varphi(x))\,dx = \sum_{\ell;T_\ell\subset\mathcal{D}_{\rm reg}} \frac{|T_\ell|}{|\mathcal{D}|} W(\nabla\varphi_{|T_\ell}),$$

where $\cup_\ell T_\ell$ is the triangulation of $\mathcal{D}_{\rm reg}$. The volume ratio $|T_\ell|/|\mathcal{D}|$ is equal to n_ℓ/N, where n_ℓ is the number of atoms included in the finite element T_ℓ, and N is the total number of atoms in the system. Besides, by definition, $W(\nabla\varphi_{|T_\ell})$ is the energy of an atom in a lattice deformed by the linear map $\nabla\varphi_{|T_\ell}$, which is exactly equal to the energy $E_\ell\left(\{\varphi^{i_\alpha}\}_{\alpha=1}^{N_r}\right)$. Hence, the first term of (5.17) reads

$$\frac{1}{|\mathcal{D}|}\int_{\mathcal{D}_{\rm reg}} W(\nabla\varphi(x))\,dx = \frac{1}{N}\sum_{\ell;T_\ell\subset\mathcal{D}_{\rm reg}} n_\ell\, E_\ell\left(\{\varphi^{i_\alpha}\}_{\alpha=1}^{N_r}\right).$$

Up to a multiplicative constant, we recover the expression (5.23) in the subdomain $\mathcal{D}_{\rm reg}$.

The QuasiContinuum method has been applied in a number of practical situations, see *e.g.* the works [140, 162, 170, 139, 13, 135] for more examples and some numerical analysis.

5.4 Some elements of analysis

We first need to mention that the mathematical and numerical study of the models of classical continuum mechanics form a scientific field in itself, before even addressing specific issues related to an atomistic coupling. We will not review here such aspects and refer the reader to, for instance, the very nice review [21]. The reader can consult [23, 141] for all issues related to quasiconvexity – a central issue in this field. In short, quasiconvexity is the natural condition on the potential W so that problem (5.4) admits a minimizer. Important issues are also examined in [82, 83, 56, 112, 142, 22]. The important *rigidity lemmas* are exposed in [101, 102, 85, 160]. For the *gradient Young measures*, a useful tool to study oscillating minimizing sequences (often present in this type of problems), we refer to [142, 156, 178].

The problem of minimizing energies coupling atomistic to continuum, like the coupled energy (5.17), brings substantial difficulties to an already quite intricate landscape. We only mention here two typical spurious effects that can arise when coupling two mathematical descriptions so different in nature as the atomistic and the continuum description. First,

it was demonstrated in a one-dimensional setting, in [36, 35], that minimizing the coupled energy can lead to inconsistencies. The appearance of a fracture in the zone described by continuum mechanics can typically energetically cost less than in the zone described by atomistic modelling. This is of course incorrect, from the modelling viewpoint, and ruins naïve adaptive strategies. The model can be amended so that the spurious effect disappears. See [36] for more details.

Another example of such difficulties is the existence of *ghost forces* at the interface between two zones modelled by two different models. The notion has been first introduced and discussed in [163], see also [67, 69, 122, 164]. The phenomenon is not present in the oversimplified case of one dimensional nearest neighbor interactions, but arises for any other interaction law, even in a one-dimensional system with second nearest neighbor interactions and no external force. The difficulty comes from the lack of balance for atoms close to the interface: some of the neighbours of such an atom can be missing (it is in the "other" zone), and an error appears. What should be an equilibrium is not, since some forces do not compensate each other. Several techniques exist to fix the flaw: *energy based* formulations and *force based* formulations (the latter consists in approximating the atomistic *forces* (rather than the *energy*)). See [122, 69, 68, 70, 72, 67].

Similar problems are encountered in the dynamics. This is reminiscent of well-known problems in, for instance, wave propagations, where dedicated methods such as perfectly matching layers (see [29, 174] for instance) and/or transparent boundary conditions are needed (see [1, 2, 109, 145]).

The above discussion certainly demonstrates that appropriately setting the problem is delicate. The definite practical success of numerical approaches involving hybrid problems should motivate further mathematical efforts. The state of the mathematical understanding is certainly lagging behind the success of the numerical simulations.

6 Micro-Macro models for complex fluids

Our final topic is the micro-macro modelling of some non-Newtonian fluids: polymeric fluids. Similarly to our previous section on solid modelling, we now present an approach that concurrently couples a mesoscopic 'statistical' description of the fluid material and a

more traditional, entirely macroscopic description. As announced in the introduction, this section is adapted from [42, 123].

6.1 Macroscopic models for fluids

To begin with, we recall here some elements on the modelling of viscous incompressible fluids. Consider a viscous fluid with volumic mass (or density) ρ, flowing at the velocity $\boldsymbol{u}$, and experiencing external forces $\boldsymbol{f}$ per unit mass. Denote by $\boldsymbol{T}$ the stress tensor. The equation of conservation of mass for the fluid reads

$$\frac{\partial \rho}{\partial t} + \operatorname{div}(\rho\,\boldsymbol{u}) = 0, \tag{6.1}$$

while the equation expressing the conservation of momentum is

$$\frac{\partial(\rho\,\boldsymbol{u})}{\partial t} + \operatorname{div}(\rho\,\boldsymbol{u}\otimes\boldsymbol{u}) - \operatorname{div}\boldsymbol{T} = \rho\boldsymbol{f}. \tag{6.2}$$

For such a viscous fluid, the stress tensor reads $\boldsymbol{T} = -p\,\mathbf{Id} + \boldsymbol{\tau}$, where p is the (hydrodynamic) pressure, and $\boldsymbol{\tau}$ is the tensor of viscous stresses. The equations are supplied with appropriate initial and boundary conditions we omit. In order to close the above set of equations, a *constitutive law* is needed, which relates the viscous stress $\boldsymbol{\tau}$ and the velocity field $\boldsymbol{u}$, namely

$$\boldsymbol{\tau} = \boldsymbol{\tau}(\boldsymbol{u}, \rho, \ldots). \tag{6.3}$$

Expression (6.3) is symbolic. A more precise formulation may involve derivatives in time, or in space, of the various fields $\boldsymbol{\tau}$, $\boldsymbol{u}$, ρ, ...

The simplest possible situation is that of *Newtonian* fluids (typically the case of water), for which, by definition, $\boldsymbol{\tau}$ linearly depends on the velocity $\boldsymbol{u}$. Under appropriate assumptions, it can then be shown that the relation between $\boldsymbol{\tau}$ and $\boldsymbol{u}$ necessarily takes the form $\boldsymbol{\tau} = \lambda(\operatorname{div}\boldsymbol{u})\,\mathbf{Id} + 2\eta\,\boldsymbol{d}$, where λ and η are the two Lamé coefficients, and $\boldsymbol{d}$ denotes the (linearized) rate of deformation tensor $\boldsymbol{d} = \frac{1}{2}(\nabla\boldsymbol{u} + \nabla\boldsymbol{u}^T)$, with the convention $(\nabla\boldsymbol{u})_{ij} = \dfrac{\partial u_i}{\partial x_j}$. The derivation proceeds, and in the case of an incompressible ($\operatorname{div}\boldsymbol{u} = 0$) homogeneous ($\rho = \rho_0$) Newtonian viscous fluid, the equations obtained are the celebrated incompressible Navier-Stokes equations

$$\left\{ \begin{array}{rcl} \rho_0 \left(\dfrac{\partial \boldsymbol{u}}{\partial t} + (\boldsymbol{u}\cdot\nabla)\,\boldsymbol{u} \right) - \eta\Delta\boldsymbol{u} + \nabla p & = & \rho_0\boldsymbol{f}, \\ \operatorname{div}\boldsymbol{u} & = & 0. \end{array} \right. \tag{6.4}$$

When the fluid is *not* Newtonian, that is, in many practically relevant situations (most of the fluids of the everyday life are indeed not Newtonian: blood, wine, oil, ...), a constitutive equation (6.3) needs to be identified. It is of course specific to the fluid under consideration. Equations (6.1)-(6.2) together with the constitutive equation (6.3) (and possibly equations for the energy and the temperature) then form the model for the fluid. For non-Newtonian fluids, many constitutive laws, and thus many purely macroscopic models, exist. All are based upon considerations of continuum mechanics. It is usual to decompose the stress tensor $\boldsymbol{\tau}$ as the sum $\boldsymbol{\tau} = \boldsymbol{\tau}_n + \boldsymbol{\tau}_p$, where $\boldsymbol{\tau}_n$ denotes the Newtonian contribution and $\boldsymbol{\tau}_p$ denotes the part of the stress (called *non-Newtonian* or extra stress) that cannot be modelled in the Newtonian manner. The bottom line is then to write an equation, in the vein of (6.3), ruling the evolution of the non-Newtonian contribution $\boldsymbol{\tau}_p$ and/or encoding a relation between the latter and other quantities characterizing the fluid dynamics, such as the deformation tensor $\boldsymbol{d}$, or $\nabla \boldsymbol{u}$ itself. One famous example is the *Oldroyd B model*, which, in non-dimensional form, writes:

$$\left\{ \begin{array}{l} \mathrm{Re} \left(\dfrac{\partial \boldsymbol{u}}{\partial t} + \boldsymbol{u} \cdot \nabla \boldsymbol{u} \right) = (1-\epsilon) \Delta \boldsymbol{u} - \nabla p + \mathrm{div}\, \boldsymbol{\tau}_p, \\ \mathrm{div}\, \boldsymbol{u} = 0, \\ \dfrac{\partial \boldsymbol{\tau}_p}{\partial t} + \boldsymbol{u} \cdot \nabla \boldsymbol{\tau}_p - (\nabla \boldsymbol{u}) \boldsymbol{\tau}_p - \boldsymbol{\tau}_p (\nabla \boldsymbol{u})^T = \dfrac{\epsilon}{\mathrm{We}} \left(\nabla \boldsymbol{u} + (\nabla \boldsymbol{u})^T \right) - \dfrac{1}{\mathrm{We}} \boldsymbol{\tau}_p. \end{array} \right. \tag{6.5}$$

The *Reynolds number* $\mathrm{Re} > 0$, the *Weissenberg number* (ratio of the characteristic relaxation time of the microstructures in the fluid to the characteristic time of the fluid) $\mathrm{We} > 0$ and $\epsilon \in (0,1)$ are the non-dimensional parameters of the model.

The Oldroyd B model is not capable of reproducing many experimentally observed behaviors. Refined macroscopic models for viscoelastic fluids have thus been derived, allowing for a better agreement between simulation and experiments. Each model correspond to a particular constitutive law. Overall, they yield better results than the Oldroyd B model, and satisfactorily agree with several prototypical experiments on simple flows. Of course, in terms of scientific computing, solving the three-field problem (6.5) is much more difficult and computationally demanding than the 'simple' Newtonian problem (6.4). However, the major *scientific* difficulty is neither a mathematical one nor a computational one. The major difficulty is to *derive* a constitutive equation (6.3). It requires a deep qualitative and quantitative understanding of the physical properties of the fluid under consideration. And

there are many fluids, and many experimental situations. For many non-Newtonian fluids, complex in nature, reaching such an understanding is therefore a challenge. Moreover, even if such an equation is approximately known, evaluating the impact of its possible flaws on the final outcome of the simulation is not an easy issue. It can only be completed *a posteriori*, comparing the results to actual experimental observations, when the latter exist, and they do not always exist. The difficulty is all the more prominent that non-Newtonian fluids are very diverse in nature.

All this, in its own rights, motivates the need for alternative strategies, based on an explicit microscopic modelling of the fluid. This gives rise to the so-called *micro-macro models*. The lack of information at the macroscopic level is then circumvented by a multiscale strategy consisting in searching for the information at a finer level (where reliable models do exist, based on general conservation equations, posed *e.g.* on the microstructures of the fluids). The latter information is then inserted in the equations of conservation at the macroscopic level.

6.2 Micro-Macro simulations of polymeric fluids

Polymeric fluids are non-Newtonian fluids. They consist of a solvent where, at the mesoscopic scale, polymeric chains float, see Figure 6. Each polymeric chain, itself possibly consisting of thousands of atoms, is admittedly well modeled using a coarse-grained description. The simplest possible such description consists in a single end-to-end vector, called a *dumbbell*, that models the total length and overall direction of the chain, see Figure 6.

Our purpose is now to explain how the derivation of an explicit constitutive law can be bypassed in this context. The success of the enterprise owes to the existence of a well established kinetic theory for solutions of polymeric chains, see the monographs [30, 31, 73, 151, 153]. The theory is based on a statistical description of the chains.

For our exposition, we pick the specific example of polymeric fluids, but the field is much wider. We mention the modelling of liquid crystals (see the reference books [73, 151], and the articles [180, 61, 84] for some mathematical and numerical studies), or suspensions (see [95, 51, 52, 53, 27]), or blood flows (see the models proposed in [79, 152]), would lead to considerations similar in spirit.

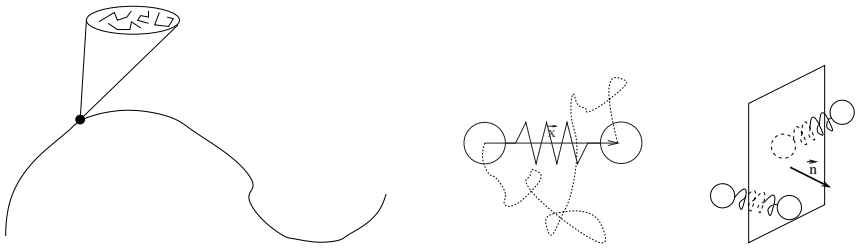

Figure 6: Left: A collection of polymeric chains lies, microscopically, at each macroscopic point of the trajectory of a fluid particle. Middle: The dumbbell model: the end-to-end vector $\boldsymbol{X}$ is the vector connecting the two beads that model the entire polymeric chain. It is supposed to accurately model the typical behaviour of the entire chain. Right: Kramer formula– the contribution of all polymeric chains to the stress is obtained summing over all chains cut by the plane considered.

Let us now denote $\psi(t, \boldsymbol{x}, \boldsymbol{r})$ the probability density for the end-to-end vector $\boldsymbol{r}$ modeling the polymer chains at macropoint $\boldsymbol{x}$ and time t. The variation of ψ follows from three different phenomena:

1. a hydrodynamic force: the dumbbell is elongated or shortened because of the interaction with the fluid; its two ends do not necessarily see the same fluid velocity, the slight difference in velocities (basically $\nabla \boldsymbol{u}(t, \boldsymbol{x})\, \boldsymbol{r}$) results in a force elongating the dumbbell $\zeta \nabla \boldsymbol{u}(t, \boldsymbol{x})\, \boldsymbol{r}$, where ζ denotes a friction coefficient;

2. an entropic force $\boldsymbol{F}$ issued from the coarse-graining procedure and which is reminiscent of the actual, much more complex, geometry of the entire polymeric chain;

3. a Brownian force, modelling the permanent collisions of the polymeric chain with solvent molecules, which (randomly) modifies its evolution.

The equation of conservation of momentum reads as the following evolution equation on ψ:

$$\begin{aligned} &\frac{\partial \psi(t, \boldsymbol{x}, \boldsymbol{r})}{\partial t} + \boldsymbol{u}(t, \boldsymbol{x}) \cdot \nabla_{\boldsymbol{x}} \psi(t, \boldsymbol{x}, \boldsymbol{r}) \\ &\quad = -\mathrm{div}_{\boldsymbol{r}} \left(\left(\nabla_{\boldsymbol{x}}\, \boldsymbol{u}(t, \boldsymbol{x})\, \boldsymbol{r} - \frac{2}{\zeta}\, \boldsymbol{F}(\boldsymbol{r}) \right) \psi(t, \boldsymbol{x}, \boldsymbol{r}) \right) + \frac{2kT}{\zeta}\, \Delta_{\boldsymbol{r}} \psi(t, \boldsymbol{x}, \boldsymbol{r}). \end{aligned} \tag{6.6}$$

Equation (6.6) is called a *Fokker-Planck equation*. The three terms of the right-hand side of (6.6) respectively correspond to the three phenomena listed above. A crucial point is that,

in this right-hand side, all differential operators acting on ψ are related to the variable $\boldsymbol{r}$ of the configuration space, *not* of the ambient physical space. In contrast, the gradient of the left-hand side is the usual transport term in the physical space $\boldsymbol{u} \cdot \nabla_{\boldsymbol{x}}$. In the absence of such a transport term (this will indeed be the case for extremely simple geometries, such as that of a Couette flow presented below), (6.6) is simply a family of Fokker-Planck equations posed in variables $(t, \boldsymbol{r})$ and *parameterized* in $\boldsymbol{x}$. These equations are coupled only through the macroscopic field $\boldsymbol{u}$. When the transport term is present, (6.6) is a genuine partial differential equation in all variables $(t, \boldsymbol{x}, \boldsymbol{r})$. It is intuitively clear that the latter case is much more difficult, computationally and mathematically.

Once ψ is obtained, its contribution to the total stress, and, further, its impact on the macroscopic flow, need to be formalized. Elementary considerations of continuum mechanics (see Figure 6) show that the contribution to the stress is given by the so-called *Kramers formula*,

$$\boldsymbol{\tau}_p(t, \boldsymbol{x}) = -n_p kT\, \mathbf{Id} + n_p \int (\boldsymbol{r} \otimes \boldsymbol{F}(\boldsymbol{r}))\, \psi(t, \boldsymbol{x}, \boldsymbol{r})\, d\boldsymbol{r}, \tag{6.7}$$

where n_p denotes the total number of polymeric chains per unit volume.

The complete system of equations combines the equation of conservation of momentum at the macroscopic level, the incompressibility constraint, the Kramers formula, and the Fokker-Planck equation for the distribution of the end-to-end vector. In non-dimensional form, it reads:

$$\left\{ \begin{array}{l} \mathrm{Re} \left(\dfrac{\partial \boldsymbol{u}}{\partial t} + (\boldsymbol{u} \cdot \nabla)\, \boldsymbol{u} \right) - (1-\epsilon)\Delta \boldsymbol{u} + \nabla p - \mathrm{div}\, \boldsymbol{\tau}_p = \boldsymbol{f}, \\ \mathrm{div}\, \boldsymbol{u} = 0, \\ \\ \boldsymbol{\tau}_p(t, \boldsymbol{x}) = \dfrac{\epsilon}{\mathrm{We}} \left(\displaystyle\int (\boldsymbol{r} \otimes \boldsymbol{F}(\boldsymbol{r}))\, \psi(t, \boldsymbol{x}, \boldsymbol{r})\, d\boldsymbol{r} - \mathbf{Id} \right), \\ \dfrac{\partial \psi(t, \boldsymbol{x}, \boldsymbol{r})}{\partial t} + \boldsymbol{u}(t, \boldsymbol{x}) \cdot \nabla_{\boldsymbol{x}} \psi(t, \boldsymbol{x}, \boldsymbol{r}) \\ \quad = -\mathrm{div}_{\boldsymbol{r}} \left(\left(\nabla_{\boldsymbol{x}}\, \boldsymbol{u}(t, \boldsymbol{x})\, \boldsymbol{r} - \dfrac{1}{2\mathrm{We}}\, \boldsymbol{F}(\boldsymbol{r}) \right) \psi(t, \boldsymbol{x}, \boldsymbol{r}) \right) + \dfrac{1}{2\mathrm{We}}\, \Delta_{\boldsymbol{r}} \psi(t, \boldsymbol{x}, \boldsymbol{r}). \end{array} \right. \tag{6.8}$$

An alternative description of the evolution of polymeric chains is provided by the stochastic viewpoint. This viewpoint is actually extremely useful in practice, because it

allows to circumvent the difficulties related to the high-dimensionality of the Fokker-Planck equation (6.6). It is indeed to be borne in mind that when the geometric description of the chain is richer than a coarse, dumbbell model, then the end-to-end vector is replaced by a possibly highly multidimensional vector, and the dimensionality of the Fokker-Planck equation grows correspondingly.

As an alternative to (6.6), we may model the mesoscopic part of the system by the set of *stochastic differential equations*:

$$d\boldsymbol{X}_t(\boldsymbol{x}) + \boldsymbol{u}(t,\boldsymbol{x})\cdot\nabla\boldsymbol{X}_t(\boldsymbol{x})\,dt = \nabla\boldsymbol{u}(t,\boldsymbol{x})\boldsymbol{X}_t(\boldsymbol{x})\,dt - \frac{2}{\zeta}\boldsymbol{F}(\boldsymbol{X}_t(\boldsymbol{x}))\,dt + 2\sqrt{\frac{kT}{\zeta}}d\boldsymbol{W}_t, \quad (6.9)$$

where $\boldsymbol{X}_t(\boldsymbol{x})$ denotes the stochastic process modeling the conformation of the polymeric chain at $\boldsymbol{x}$ at time t. The stress is then given by

$$\boldsymbol{\tau}_p(t,\boldsymbol{x}) = n_p\Big(\mathbb{E}(\boldsymbol{X}_t(\boldsymbol{x})\otimes\boldsymbol{F}(\boldsymbol{X}_t(\boldsymbol{x}))) - kT\mathbf{Id}\Big), \quad (6.10)$$

where n_p is the concentration of polymers. The coupled system is thus:

$$\begin{cases} \mathrm{Re}\left(\dfrac{\partial\boldsymbol{u}}{\partial t} + \boldsymbol{u}\cdot\nabla\boldsymbol{u}\right) - (1-\epsilon)\Delta\boldsymbol{u} + \nabla p = \mathrm{div}\,\boldsymbol{\tau}_p + \boldsymbol{f}, \\ \mathrm{div}\,\boldsymbol{u} = 0, \\ \boldsymbol{\tau}_p = \dfrac{\epsilon}{\mathrm{We}}\Big(\mathbb{E}(\boldsymbol{X}_t\otimes\boldsymbol{F}(\boldsymbol{X}_t)) - \mathbf{Id}\Big), \\ d\boldsymbol{X}_t + \boldsymbol{u}\cdot\nabla\boldsymbol{X}_t\,dt = \nabla\boldsymbol{u}\boldsymbol{X}_t\,dt - \dfrac{1}{2\mathrm{We}}\boldsymbol{F}(\boldsymbol{X}_t)\,dt + \dfrac{1}{\sqrt{\mathrm{We}}}d\boldsymbol{W}_t. \end{cases} \quad (6.11)$$

In both the above systems (6.8) and (6.11), the force $\boldsymbol{F}$ needs to be made specific. In full generality, it is assumed of the form $\boldsymbol{F}(\boldsymbol{X}) = \pi'(\|\boldsymbol{X}\|)\dfrac{\boldsymbol{X}}{\|\boldsymbol{X}\|}$, for a given potential π. The simplest potential π is the quadratic potential $\pi_{\mathrm{Hook}}(l) = H\dfrac{l^2}{2}$. A peculiarity of this choice is that the multiscale model is then equivalent to the Oldroyd B model (6.5). Other choices of forces allow to capture important physical behaviours and yield models that are genuinely multiscale: the *FENE* force corresponding to the potential $\pi_{\mathrm{FENE}}(l) = -\dfrac{bkT}{2}\ln\left(1 - \dfrac{l^2}{bkT/H}\right)$ is the most commonly used type of such forces. In general, it is believed that a multiscale model is more accurate than a purely macroscopic model, and that the description of the microstructure need not be sophisticated to give excellent results, capturing the right qualitative physics being the only important issue (see the FENE force in contrast to the Hookean force).

6.3 Numerical approaches

We now turn to the discretization of the systems (6.8) or (6.11). Most of the numerical methods employed for the simulation of non Newtonian fluids are based upon a finite element discretization in space and Euler schemes in time, using a semi-explicit scheme: at each timestep, the velocity is first solved for a given stress, and then the stress is updated, for the corresponding velocity.

Three types of difficulties typically arise:

1. An *inf-sup condition* must be satisfied by the spaces respectively used for the discrete velocity, the pressure and the stress (in order for the discretization to be stable for ϵ close to 1).

2. The *advection terms* need to be appropriately discretized, in the equation of conservation of momentum, in the equation on $\boldsymbol{\tau}_p$ in (6.5), in the equation on ψ in (6.8), on in the SDE in (6.11).

3. The *nonlinear terms* require, as always, special attention. On the one hand, some nonlinear terms stem from the coupling: $\nabla \boldsymbol{u}\boldsymbol{\tau}_p + \boldsymbol{\tau}_p(\nabla \boldsymbol{u})^T$ in (6.5), $\nabla \boldsymbol{u}\boldsymbol{X}_t$ in (6.11) or $\mathrm{div}_{\boldsymbol{r}}(\nabla \boldsymbol{u}\,\boldsymbol{r}\,\psi(t,\boldsymbol{x},\boldsymbol{r}))$ in (6.8). On the other hand, for rheological models more complicated than the Oldroyd-B or Hookean dumbbell models, some nonlinear terms come from the model itself (see the entropic force $\boldsymbol{F}(\boldsymbol{X}_t)$ in (6.11) for FENE models for example).

Besides, for both micro-macro models and purely macroscopic models, one central difficulty of the simulation of viscoelastic fluids is the so-called *High Weissenberg Number Problem* (HWNP), see for instance [110, 111]. It is indeed observed that numerical simulations do not converge when We is too large and that the problem gets all the more delicate as the mesh is refined.

Because the reader might be more familiar with a purely deterministic formulation, we begin by outlining the numerical approach for problems of type (6.8). The discretization of the Fokker-Planck equation in (6.8) is typically performed using spectral methods (see [133, 167, 113]). It is not easy to find a suitable variational formulation of the Fokker-Planck equation, and an appropriate discretization that satisfies the natural constraints on

the probability density ψ (namely non negativity, and normalization). We refer to [55, 134] for suitable discretizations in the FENE case. A major difficulty is the possible high dimensionality of the Fokker-Planck equation. In the context of polymeric fluid flow simulation, when the polymer chain is modelled by a chain of $N+1$ beads linked by N springs, the Fokker-Planck equation is a parabolic equation posed on a $3N$-dimensional domain. Some numerical methods have been developed to discretize such high dimensional problems. The idea is to use an appropriate Galerkin basis, whose dimension remains limited when dimension grows. We refer to [66, 177, 50] for the sparse-tensor product approach, to [136, 114] for the reduced basis approach and to [6, 7, 124] for a method coupling a sparse-tensor product discretization with greedy algorithms used in approximation theory.

The numerical approach for the coupled system (6.11) involving the stochastic differential equations formulation is different. A Monte Carlo method is employed to discretize the expectation: at each macroscopic point $\boldsymbol{x}$ (*i.e.* at each node of the mesh once the problem is discretized), many replicas (or realizations) $(\boldsymbol{X}_t^{k,K})_{1\leq k\leq K}$ of the stochastic process $\boldsymbol{X}_t$ are simulated, driven by independent Brownian motions $(\boldsymbol{W}_t^k)_{k\geq 1}$, and the stress tensor is obtained as an empirical mean over these processes:

$$\boldsymbol{\tau}_p^K = \frac{\epsilon}{\mathrm{We}}\left(\frac{1}{K}\sum_{k=1}^{K}\boldsymbol{X}_t^{k,K}\otimes\boldsymbol{F}(\boldsymbol{X}_t^{k,K})-\mathbf{Id}\right).$$

In this context, the discretization method coupling a finite element method and a Monte Carlo technique is called CONNFFESSIT for *Calculation Of Non-Newtonian Flow: Finite Elements and Stochastic SImulation Technique* (see [115]). We describe below the implementation of this method in a simple geometry.

To give a flavour of the numerical difficulties involved when solving coupled problems of the type (6.8) or (6.11), we momentarily consider the simple situation of a start-up Couette flow (see Figure 7). The fluid flows between two parallel planes. Such a model is typically obtained considering a flow in a rheometer, between two cylinders, and taking the limit of large radii for both the inner and the outer cylinders (see Figure 7). At initial time, the fluid is at rest. The lower plane ($y=0$, modelling the inner cylinder of the rheometer) is then shifted with a velocity $V(t)$, which, for simplicity, will be set to a constant value V (sinusoidal velocities may also be applied). On the other hand, the upper plane ($y=L$,

modelling the outer cylinder of the rheometer) is kept fixed. Such a setting is called a *start-up flow*, and because it is confined between two parallel planes, a *Couette flow*.

We denote by x and y the horizontal and vertical axes, respectively. The flow is assumed invariant in the direction perpendicular to (x, y).

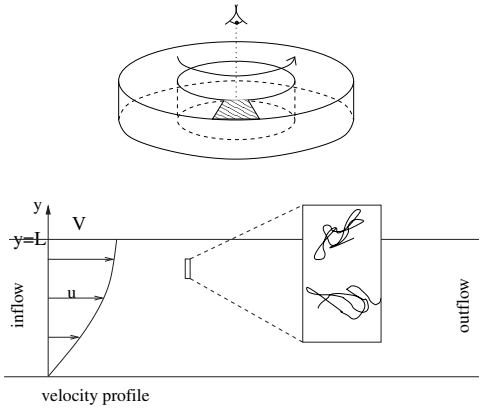

Figure 7: Schematic representation of a rheometer. On an infinitesimal angular portion, seen from above, the flow is a simple shear flow (Couette flow) confined between two planes with velocity profile $(u(t, y), 0, 0)$.

After appropriate assumptions (the flow is laminar, the velocity writes $\boldsymbol{u} = u(t, y)\, \boldsymbol{e}_x$, the entropic force is taken Hookean, etc), the coupled system (6.8) simplifies into

$$\begin{cases} \mathrm{Re}\,\dfrac{\partial u}{\partial t}(t,y) = (1-\epsilon)\dfrac{\partial^2 u}{\partial y^2}(t,y) + \dfrac{\partial \tau}{\partial y}(t,y), \\ \tau(t,y) = \dfrac{\epsilon}{\mathrm{We}} \displaystyle\int_{\mathbb{R}^2} P\,Q\,\psi(t,y,P,Q)\,dP\,dQ, \\ \dfrac{\partial \psi}{\partial t}(t,y,P,Q) = -\dfrac{\partial}{\partial P}\left(\left(\dfrac{\partial u}{\partial y}(t,y)Q - \dfrac{1}{2\mathrm{We}}P\right)\psi(t,y,P,Q)\right) \\ \qquad +\dfrac{\partial}{\partial Q}\left(\dfrac{1}{2\mathrm{We}}Q\ \psi(t,y,P,Q)\right) + \dfrac{1}{2\mathrm{We}}\left(\dfrac{\partial^2}{\partial P^2} + \dfrac{\partial^2}{\partial Q^2}\right)\psi(t,y,P,Q), \end{cases} \tag{6.12}$$

where P and Q are the two components of the end-to-end vector $\boldsymbol{r}$, along the x and y axes respectively. In the above system, $\tau(t, y)$ denotes the xy entry of the tensor $\boldsymbol{\tau}_p$. Actually, the pressure field, and the other entries of the stress tensor may be then deduced, independently.

We emphasize at this stage the tremendous simplifications that the Couette model allows for. Owing to the simple geometric setting and the fact that the flow is assumed laminar, the divergence-free constraint (6.8) is fulfilled by construction of the velocity field and can be eliminated from the system. In addition, both transport terms $(\boldsymbol{u}\cdot\nabla)\boldsymbol{u}$ and $(\boldsymbol{u}\cdot\nabla)\psi$ vanish, again because of evident geometrical considerations. This explains the extremely simple form of the equation of conservation of momentum in this context, which indeed reduces to a simple one-dimensional heat equation. This set of simplifications is specific to the Couette flow. Substantial difficulties arise otherwise.

The macroscopic equation is discretized with finite elements: P1 finite elements for the velocity and P0 finite elements for the stress tensor.

If the mesoscopic scale is modelled by the Fokker-Planck equation, the latter may be discretized using finite difference in time (taking explicit the transport term and implicit the parabolic terms) and a spectral method for the space variable. More precisely, we first introduce the equilibrium solution for the last line of (6.12) when $u = 0$, namely $\psi_\infty(P,Q) = \dfrac{1}{2\pi}\exp\left(-\dfrac{P^2+Q^2}{2}\right)$, rewrite the Fokker-Planck equation using $\varphi = \dfrac{\psi}{\psi_\infty}$ as the primary unknown function, and next proceed with the discretization. Because of the specific form of ψ_∞, the most appropriate Galerkin basis consists of (tensor products of) Hermite polynomials H_i, which indeed satisfy $\dfrac{1}{\sqrt{2\pi}}\displaystyle\int_{\mathbb{R}} H_i(P)H_j(P)\exp\left(-P^2/2\right)dP = \delta_{ij}$. Note that the use of such a spectral basis allows to circumvent the practical difficulty related to the fact that the equation is posed on the whole space.

Alternatively to the last two lines of (6.12), the mesoscopic scale may be modelled using the stochastic differential equations

$$\left\{\begin{array}{l} dP(t,y) = \left(\dfrac{\partial u}{\partial y}(t,y)Q(t) - \dfrac{1}{2\mathrm{We}}P(t,y)\right)dt + \dfrac{1}{\sqrt{\mathrm{We}}}\,dV_t, \\ dQ(t) = -\dfrac{1}{2\mathrm{We}}Q(t)dt + \dfrac{1}{\sqrt{\mathrm{We}}}\,dW_t, \end{array}\right. \tag{6.13}$$

where V_t and W_t are two mutually independent one-dimensional Brownian motions, and the stress is given by

$$\tau(t,y) = \frac{\epsilon}{\mathrm{We}}\int_{\mathbb{R}^2} P\,Q\,\psi(t,y,P,Q)\,dP\,dQ = \frac{\epsilon}{\mathrm{We}}\,\mathbb{E}(P(t,y)Q(t)). \tag{6.14}$$

The system is discretized using a forward Euler scheme in time and a standard Monte-Carlo

method for replacing the above expectation value by an empirical mean:

$$P_{i,k}^{n+1} = \Delta t \frac{U_i^{n+1} - U_{i-1}^{n+1}}{\Delta y} Q_k^n + \left(1 - \frac{\Delta t}{2\mathrm{We}}\right) P_{i,k}^n + \sqrt{\frac{\Delta t}{\mathrm{We}}} V_k^n, \tag{6.15}$$

$$Q_k^{n+1} = \left(1 - \frac{\Delta t}{2\mathrm{We}}\right) Q_k^n + \sqrt{\frac{\Delta t}{\mathrm{We}}} W_k^n, \tag{6.16}$$

for $1 \leq k \leq K$ (number of realizations of the random variables), where V_k^n and W_k^n are independent normal random variables, and

$$(\tau^h)_i^{n+1} = \frac{\epsilon}{\mathrm{We}} \frac{1}{K} \sum_{k=1}^{K} P_{i,k}^{n+1} Q_k^{n+1}. \tag{6.17}$$

This discretization is the CONNFFESSIT approach mentioned above, implemented in a simple case.

A crucial remark (which not only applies to the Couette flow, but also to more general situations) is the following. Since the stress $(\tau^h)_i^{n+1}$ is an empirical mean (6.17), it is thus *also a random variable*. It follows that the discretized macroscopic velocity itself is a random variable. In contrast, at the continuous level, $K \to \infty$ in (6.17), and the stress and the velocity are both deterministic quantities (since the expectation value is a deterministic quantity). Consequently, computing the velocity or the stress using the stochastic approach implies performing a *collection* of simulations, and averaging out the results. This immediately brings variance issues into the picture. Appropriate variance reduction methods can be applied. We refer to [123, 103].

The Matlab codes corresponding to the above description are available at

`http://hal.inria.fr/inria-00165171`

The numerical approach to treat other types of entropic forces (like the FENE force) and other geometries of flows follows the same line, but the extension can be quite involved, especially for the Fokker-Planck approach.

It is evident from the above discussion that the work load implied by such a coupling may be overwhelming in many practical, especially three-dimensional, situations. Thus the micro-macro simulations are, to date, limited in applications. They serve as a backroom strategy to validate or derive appropriate constitutive laws. They may also be employed on a limited portion of the computational domain (typically in a layer close to the boundaries

where non-Newtonian effects are expectedly important; see for example [78] for results in this direction).

6.4 Elements of mathematical and numerical analysis

The questions raised by the above multiscale models in terms of mathematical analysis and numerical analysis are diverse in nature, because the mathematical objects involved are themselves diverse. The situation can of course not be expected to be simpler than, say, models like the Oldroyd B model (6.5). There is a two-fold reason for this. Firstly, the multiscale models are indeed, for some simple particular cases, equivalent to some single-scale models. We have mentioned the Hookean model equivalent to the Oldroyd B model. Secondly, multiscale systems at least involve macroscopic equations, either because they couple general equations of conservation (like the first two lines of (6.8)) with equations at finer scales, or because they use in practice two different sets of equations in different regions of the computational domain, and one of such set of equations is often purely macroscopic. Without even speaking of the coupling issues, considering separately each region, or each equation, is necessary.

Mathematical analysis Systems like (6.5) modelling purely macroscopically non-Newtonian fluids typically include the Navier-Stokes equations, with the additional term $\mathrm{div}\, \boldsymbol{\tau}_p$ in the right-hand side. The equation on $\boldsymbol{\tau}_p$ is essentially a transport equation and, formally, $\boldsymbol{\tau}_p$ has at best the regularity of $\nabla \boldsymbol{u}$ (this formal observation is important for the choice of appropriate functional spaces for the mathematical setting, and of the discretization spaces for numerical methods). The term $\mathrm{div}\, \boldsymbol{\tau}_p$ in the right-hand side of the momentum equation is not likely to bring more regularity on $\boldsymbol{u}$. It is thus expected that the study of these coupled systems contains at least the well-known difficulties of the Navier-Stokes equations. Recall that for the three-dimensional Navier-Stokes equations, it is known that global-in-time weak solutions exist but the regularity, and thus the uniqueness, of such solutions for appropriate data is only known locally in time.

Besides the difficulties already contained in the Navier-Stokes equations (which essentially originate from the Navier term $\boldsymbol{u} \cdot \nabla \boldsymbol{u}$), the coupling with the equation on $\boldsymbol{\tau}_p$ raises additional problems. First, these equations contain a transport term $\boldsymbol{u} \cdot \nabla \boldsymbol{\tau}_p$ without any

diffusion term in the space variable. They are hyperbolic in nature. The regularity on the velocity $\boldsymbol{u}$ is typically not sufficient to rigorously treat this transport term by a characteristic method. Moreover, these equations involve a nonlinear multiplicative term $\nabla \boldsymbol{u}\ \boldsymbol{\tau}_p$. Finally, for the most sophisticated models, the equations defining $\boldsymbol{\tau}_p$ generally contain additional non-linearities. These difficulties of course limit the state-of-the-art mathematical well-posedness analysis to mainly *local-in-time* existence and uniqueness results. They also have many implications on the numerical methods (in terms of choice of the discretization spaces, stability of the numerical schemes, ...).

Many examples of results for such macroscopic models may be found in the literature. See, for instance, [157, 91, 92, 80, 127, 130, 159, 80].

For multiscale models, the study has begun with the early work [158]. There is now a growing literature on such models, presumably because they are prototypical of a broad class of multiscale models, where some parameters inserted in the macroscopic equations are computed using models at finer scales.

The difficulties present for the purely macroscopic models discussed above are also present *mutatis mutandis* in the multiscale models. They are related to the *transport terms* (in addition to $\boldsymbol{u} \cdot \nabla \boldsymbol{u}$, we now have $\boldsymbol{u} \cdot \nabla \boldsymbol{X}_t$ and $\boldsymbol{u} \cdot \nabla \psi$), the *nonlinear terms* either coming from the coupling between variables (in addition to the variables $(\boldsymbol{u}, p)$ and $\boldsymbol{\tau}_p$, we now have $\nabla \boldsymbol{u} \boldsymbol{X}_t$ and $\mathrm{div}_{\boldsymbol{r}} (\nabla \boldsymbol{u}\, \boldsymbol{r}\, \psi)$), or inherently contained in the equations defining $\boldsymbol{\tau}_p$ (due to the non-linear entropic force $\boldsymbol{F}$).

The list of contributions include, for the coupled system involving the Fokker-Planck equation: [125, 181, 128, 24, 25, 26, 182, 131, 137, 129, 59, 60, 62]. Note the recent global existence result obtained in [138]. For the system (6.11) using the stochastic differential equation: [115, 46, 92, 74].

Perhaps the more striking fact for the theoretical analysis of the all these problems is that, in contrast to the situation of "standard" fluids, where *energy estimates* provide all the estimations needed, here *free energy estimates* need to be employed. Indeed, a standard formal manipulation on this system, involving some elements of stochastic calculus, yields

the following quite standard a priori estimate:

$$\frac{\mathrm{Re}}{2}\frac{d}{dt}\int_{\mathcal{D}}|\boldsymbol{u}|^2(t,\boldsymbol{x})+(1-\epsilon)\int_{\mathcal{D}}|\nabla\boldsymbol{u}|^2(t,\boldsymbol{x})+\frac{\epsilon}{\mathrm{We}}\frac{d}{dt}\int_{\mathcal{D}}\mathbb{E}(\Pi(\boldsymbol{X}_t(\boldsymbol{x})))$$
$$+\frac{\epsilon}{2\mathrm{We}^2}\int_{\mathcal{D}}\mathbb{E}(\|\boldsymbol{F}(\boldsymbol{X}_t(\boldsymbol{x}))\|^2)=\frac{\epsilon}{2\mathrm{We}^2}\int_{\mathcal{D}}\Delta\Pi(\boldsymbol{X}_t(\boldsymbol{x})), \tag{6.18}$$

where Π is the potential of the force $\boldsymbol{F}=\nabla\Pi$. Notice that the right-hand side of this equality is typically a positive term (recall that, in practice, the potential Π is convex). The situation is different from the usual a priori estimates for, say, the Navier-Stokes equations where the right-hand side is zero. Here, some energy is brought to the system by the finer scales. On finite time intervals, this is however not a difficulty for the mathematical analysis.

A typical result is, in the case of Hookean dumbbells in a shear flow, the global-in-time existence and uniqueness result proved for the first time in [106]. The solution $(u,\boldsymbol{X}_t)$ on the interval $[0,T]$ satisfies the estimate

$$\|u\|^2_{L^\infty_t(L^2_y)}+\|u\|^2_{L^2_t(H^1_{0,y})}+\|\boldsymbol{X}_t\|^2_{L^\infty_t(L^2_y(L^2_\omega))}+\|\boldsymbol{X}_t\|^2_{L^2_t(L^2_y(L^2_\omega))}$$
$$\leq C\left(\|\boldsymbol{X}_0\|^2_{L^2_y(L^2_\omega)}+\|u_0\|^2_{L^2_y}+T+\|f\|^2_{L^1_t(L^2_y)}\right).$$

This setting (Hookean dumbbell in a shear flow) is actually extremely specific. A global-in-time existence and uniqueness result is obtained since the coupling term $\nabla\boldsymbol{u}\boldsymbol{X}_t$ of the original problem simplifies to $\frac{\partial u}{\partial y}Q_t$, where Q_t is known independently of (u,P_t). In other words, this coupling term is, serendipitously, no more nonlinear.

More general studies are presented in [105, 107, 75, 44]. See also [120, 121] for related issues.

On the other hand, the presence of an energy source, the right-hand side of (6.18), affects the analysis of the long-time behaviour, like questions related to return to equilibrium. For such questions, the appropriate notion to introduce is that of *free energy* rather than *energy*. Assume zero Dirichlet boundary conditions on the velocity $\boldsymbol{u}$. The expected stationary state (equilibrium) is

$$\boldsymbol{u}(\infty,\boldsymbol{x})=0,\quad \psi(\infty,\boldsymbol{x},\boldsymbol{X})=\psi_{\mathrm{eq}}(\boldsymbol{X})\propto\exp(-\Pi(\boldsymbol{X})).$$

The free energy

$$F(t)=\frac{\mathrm{Re}}{2}\int_{\mathcal{D}}|\boldsymbol{u}|^2(t,\boldsymbol{x})+\frac{\epsilon}{\mathrm{We}}\int_{\mathcal{D}}\int_{\mathbb{R}^d}\psi(t,\boldsymbol{x},\boldsymbol{X})\ln\left(\frac{\psi(t,\boldsymbol{x},\boldsymbol{X})}{\psi_{\mathrm{eq}}(\boldsymbol{X})}\right),$$

sum of the kinetic energy plus the relative entropy with respect to the equilibrium $\psi_{\rm eq}$, can be shown to satisfy:

$$\frac{dF}{dt} = -(1-\epsilon)\int_{\mathcal{D}} |\nabla \boldsymbol{u}|^2(t,\boldsymbol{x}) - \frac{\epsilon}{2\mathrm{We}^{\,2}}\int_{\mathcal{D}}\int_{\mathbb{R}^d} \psi(t,\boldsymbol{x},\boldsymbol{X}) \left|\nabla_{\boldsymbol{X}} \ln\left(\frac{\psi(t,\boldsymbol{x},\boldsymbol{X})}{\psi_{\rm eq}(\boldsymbol{X})}\right)\right|^2. \quad (6.19)$$

Comparing with (6.18), we observe that the introduction of the entropy allows to eliminate the positive right-hand side. Standard techniques of kinetic theory (like Logarithmic Sobolev inequalities, see [12]) allow then to conclude that, under appropriate conditions, the fluid returns to equilibrium after perturbations. We refer to [104, 14]. The *multimaths* character of the setting is evident.

We would like to also mention that these estimates on the micro-macro system can be used as a guideline to derive new estimates on related macro-macro models (see [98]) and also to derive new approximation schemes (see [49]). This is an interesting (perhaps general) byproduct of mathematical studies of multiscale systems to actually contribute to better understand and approximate the associated purely macroscopic models.

Numerical analysis. Of course, the difficulties raised by the discretization of the models are, as always, reminiscent of the difficulties of the mathematical analysis. Here again, as mentioned above, the treatment of the multiscale problem necessarily requires a good knowledge of the treatment of the purely macroscopic model. An overview of the numerical difficulties encountered when simulating purely macroscopic models for non Newtonian fluids may be found in [110, 17, 153]. As for multiscale problems, we will only, for brevity, address here the stochastic formulation of the equations, that is, system (6.11). A typical result of numerical analysis, proved in [106, 74], deals with Hookean dumbbells in a shear flow. The error estimate for the discretization approach reads:

$$\left|\left|u(t_n) - \overline{u}_h^n\right|\right|_{L^2_y(L^2_\omega)} + \left|\left|\mathbb{E}(P_{t_n}Q_{t_n}) - \frac{1}{K}\sum_{k=1}^{K} P_{i,k}^n Q_k^n\right|\right|_{L^1_y(L^1_\omega)} \leq C\left(\Delta y + \Delta t + \frac{1}{\sqrt{K}}\right).$$

The main difficulties for the proof originate from the following facts:

- The velocity u_h^n is a *random variable*. The energy estimate at the continuous level cannot be directly translated into an energy estimate at the discrete level (which in turn would yield the stability of the scheme).

- The end-to-end vectors $(P^n_{i,k}, Q^n_k)_{1\leq k\leq K}$ are *coupled* random variables (even though the driving Brownian motions $(V^n_k, W^n_k)_{1\leq k\leq K}$ are independent).

- The stability of the numerical scheme requires an almost sure bound on Q^n_k.

For an extension of these results to a more general geometry and discretization by a finite difference scheme, we refer to [126]. A convergence result in space and time may be found in [43]. Many other studies now exist in the literature.

Acknowledgements

Several of the works mentioned here are joint works and the author of course acknowledges the help of his many co-authors. The author also thanks them for a critical reading of the manuscript (or one of its earlier version) and for allowing the use of some material contained in previously published co-authored works.

The research of the author is partially supported by ONR under Grant 00014-09-1-0470, and by EOARD under Grant FA8655-10-M-4002.

References

[1] Y. Achdou, C. Sabot, and N. Tchou, *Transparent boundary conditions for a class of boundary value problems in some ramified domains with a fractal boundary,* J. Comp. Phys. **220** (2007), 712–739.

[2] U.E. Aladl, A.S. Deakin, and H. Rasmussen, *Nonreflecting boundary condition for the wave equation,* J. Comput. Appl. Math. **138** (2002), 309–323.

[3] G. Allaire, *Homogenization and two-scale convergence*, SIAM J. Math. Anal. **23** (6), pp 1482–1518, 1992.

[4] G. Allaire, **Shape optimization by the homgenization method**, Applied Mathematical Sciences, 146, Springer, 2002.

[5] G. Allaire and S. Gutierrez, Optimal design in small amplitude homogenization, *Math. Model. Numer. Anal. (M2AN)*, 41(3):543–574, 2007.

[6] A. Ammar, B. Mokdad, F. Chinesta, and R. Keunings, *A new family of solvers for some classes of multidimensional partial differential equations encountered in kinetic theory modeling of complex fluids*, J. Non-Newtonian Fluid Mech. **139** (2006), 153–176.

[7] A. Ammar, B. Mokdad, F. Chinesta, and R. Keunings, *A new family of solvers for some classes of multidimensional partial differential equations encountered in kinetic theory modeling of complex, part II: Transient simulation using space-time separated representations*, J. Non-Newtonian Fluid Mech., **144** (2007), 98–121.

[8] A. Anantharaman, C. Le Bris, *Homogénéisation d'un matériau périodique faiblement perturbé aléatoirement*, [Homogenization of a weakly randomly perturbed periodic material], Note aux Comptes Rendus de l'Académie des Sciences, 348 (2010), 529-534.

[9] A. Anantharaman, C. Le Bris, *A numerical approach related to defect-type theories for some weakly random problems in homogenization*, submitted to SIAM MMS, `http://arxiv.org/abs/1005.3910`

[10] A. Anantharaman, C. Le Bris, *Elements of mathematical foundations for a numerical approach for weakly random homogenization problems*, submitted to Communications in Computational Physics, `http://arxiv.org/abs/1005.3922`

[11] A. Anantharaman, Thèse de l' Université Paris Est, Ecole des Ponts, in preparation.

[12] C. Ané, S. Blachère, D. Chafaï, P. Fougères, I. Gentil, F. Malrieu, C. Roberto, and G. Scheffer, "Sur les inégalités de Sobolev logarithmiques", Société Mathématique de France, 2000. In French.

[13] M. Anitescu, D. Negrut, P. Zapol, and A. El-Azab, *A note on the regularity of reduced models obtained by nonlocal quasi-continuum-like approach*, Mathematical Programming **118** (2009), 207–236.

[14] A. Arnold, J.A. Carrillo, and C. Manzini, *Refined long-time asymptotics for some polymeric fluid flow models*, Commun. Math. Sci. **8** (2010).

[15] M. Avellaneda and F. H. Lin, Compactness methods in the theory of homogenization, *Comm. Pure Appl. Math.* 40:803–847, 1987.

[16] M. Avellaneda and F. H. Lin, *L^p bounds on singular integrals in homogenization*, Comm. Pure Appl. Math. 44:897–910, 1991.

[17] F.P.T. Baaijens, *Mixed finite element methods for viscoelastic flow analysis: a review*, J. Non-Newtonian Fluid Mech. **79** (1998), 361–385.

[18] I. Babuska, B. Andersson, P. J. Smith, and K. Levin, Damage analysis of fiber composites. Part I: Statistical analysis on fiber scale, *Comput. Methods Appl. Mech. Engrg.*, 172:27–77, 1999.

[19] Bal, G., Garnier, J., Motsch, S., and Perrier, V., *Random integrals and correctors in homogenization*, Asymptot. Anal. 59 (2008), no. 1-2, 1–26.

[20] G. Bal, *Central limits and homogenization in random media*, Multiscale Model. Simul. **7** (2008), no. 2, 677–702.

[21] J. M. Ball, *Some open problems in elasticity*, in "Geometry, Mechanics, and Dynamics", Springer (2002), 3–59.

[22] J. M. Ball and R. D. James, *Fine phase mixtures as minimizers of energy*, Arch. Rat. Mech. Anal. **100** (1987), 13–52.

[23] J. M. Ball and F. Murat, *$W^{1,p}$-quasiconvexity and variational problems for multiple integrals*, J. Funct. Anal. **58** (1984), 225–253.

[24] J.W. Barrett, C. Schwab, and E. Süli, *Existence of global weak solutions for some polymeric flow models*, Math. Models and Methods in Applied Sciences **15** (2005), 939–983.

[25] J.W. Barrett and E. Süli, *Existence of global weak solutions to kinetic models for dilute polymers*, Multiscale Model. Simul. **6** (2007), 506–546.

[26] J.W. Barrett and E. Süli, *Existence and equilibration of global weak solutions to finitely extensible nonlinear bead-spring chain models for dilute polymers*, preprint, `http://web.comlab.ox.ac.uk/people/endre.suli/barrett-and-suli.2010.pdf`

[27] M. Ben Alaya and B. Jourdain, *Probabilistic approximation of a nonlinear parabolic equation occuring in rheology*, Journal of Applied Probability **44** (2007), 528–546.

[28] A. Bensoussan, J. L. Lions, G. Papanicolaou, **Asymptotic analysis for periodic structures,** Studies in Mathematics and its Applications, 5. North-Holland Publishing Co., Amsterdam-New York, 1978.

[29] J.-P. Bérenger, *A perfectly matched layer for the absorption of electromagnetic waves,* J. Comp. Phys. **114** (1994), 185–200.

[30] R.B. Bird, R.C. Armstrong, and O. Hassager, **Dynamics of polymeric liquids**, volume 1, Wiley Interscience (1987).

[31] R.B. Bird, C.F. Curtiss, R.C. Armstrong, and O. Hassager, **Dynamics of polymeric liquids**, volume 2, Wiley Interscience (1987).

[32] X. Blanc, R. Costaouec, C. Le Bris, F. Legoll, *Variance reduction in stochastic homogenization using antithetic variables*, Markov Processes and Related Fields, submitted.

[33] X. Blanc, R. Costaouec, C. Le Bris, F. Legoll, *Variance reduction in stochastic homogenization: the technique of antithetic variables*, Proceedings of a workshop at BIRS, Springer Lecture Notes in Computational Science and Engineering, submitted.

[34] X. Blanc and C. Le Bris, Improving on computation of homogenized coefficients in the periodic and quasi-periodic settings, *Netw. Heterog. Media*, **5** (1): 1–29, 2010.

[35] X. Blanc, C. Le Bris, and F. Legoll, *Analysis of a prototypical multiscale method coupling atomistic and continuum mechanics: the convex case*, Acta Math. Appl. Sinica, **23** (2007), 209–216.

[36] X. Blanc, C. Le Bris, and F. Legoll, *Analysis of a prototypical multiscale method coupling atomistic and continuum mechanics*, Math. Mod. Num. Anal. (M2AN), **39** (2005), 797–826.

[37] X. Blanc, C. Le Bris, and P.-L. Lions, *Atomistic to continuum limits for computational materials science,* Math. Mod. Num. Anal. (M2AN), **41** (2007), 391–426.

[38] X. Blanc, C. Le Bris, and P.-L. Lions, *A definition of the ground state energy for systems composed of infinitely many particles*, Comm. P.D.E, **28** (2003), 439–475.

[39] X. Blanc, C. Le Bris, and P.-L. Lions, *On the energy of some microscopic stochastic lattices*, Arch. Rat. Mech. Anal. **184** (2007), 303-339.

[40] X. Blanc, C. Le Bris, and P.-L. Lions, *Stochastic homogenization and random lattices*, Journal de Mathématiques Pures et Appliquées, **88** (2007), 34-63.

[41] X. Blanc, C. Le Bris, P.-L. Lions, *Une variante de la théorie de l'homogénéisation stochastique des opérateurs elliptiques [A variant of stochastic homogenization theory for elliptic operators]*, C. R. Acad. Sci. Série I, **343**, pp 717–724, 2006.

[42] X. Blanc, C. Le Bris, F. Legoll, T. Lelièvre, *Beyond multiscale and multiphysics: multimaths for model coupling*, to appear in Networks and heterogeneous media.

[43] A. Bonito, Ph. Clément, and M. Picasso, *Finite element analysis of a simplified stochastic Hookean dumbbells model arising from viscoelastic flows*, M2AN Math. Model. Numer. Anal., **40** (2006), 785–814.

[44] A. Bonito, Ph. Clément, and M. Picasso, *Mathematical analysis of a stochastic simplified Hookean dumbbells model arising from viscoelastic flow*, J. Evol. Equ. **6** (2006), 381–398.

[45] M. F. Ben Hassen and E. Bonnetier, An asymptotic formula for the voltage potential in a perturbed ε-periodic composite medium containing misplaced inclusions of size ε, *Proc. R. Soc. Edinb., Sect. A*, 136:669–700, 2006.

[46] J. Bonvin and M. Picasso, *Variance reduction methods for CONNFFESSIT-like simulations*, J. Non-Newtonian Fluid Mech. **84** (1999), 191–215.

[47] A. Bourgeat and A. Piatnitski, Approximation of effective coefficients in stochastic homogenization, *Ann I. H. Poincaré - PR*, **40** (2):153–165, 2004.

[48] A. Bourgeat and A. Piatnitski,, *Estimates in probability of the residual between the random and the homogenized solutions of one-dimensional second-order operator*, Asymptotic Analysis, 21, 1999, 3-4, 303–315

[49] S. Boyaval, T. Lelièvre and C. Mangoubi, *Free-energy-dissipative schemes for the Oldroyd-B model,* Math. Mod. Num. Anal. (M2AN), **43** (2009), 523–561.

[50] H.-J. Bungartz and M. Griebel, *Sparse grids*, Acta Numer. **13** (2004), 147–269.

[51] E. Cancès, I. Catto, and Y. Gati, *Mathematical analysis of a nonlinear parabolic equation arising in the modelling of non-Newtonian flows*, SIAM J. Math. Anal. **37** (2005), 60–82.

[52] E. Cancès, I. Catto, Y. Gati, and C. Le Bris, *A micro-macro model describing Couette flows of concentrated suspensions*, Multiscale Model. Simul. **4** (2005), 1041–1058.

[53] E. Cancès and C. Le Bris, *Convergence to equilibrium of a multiscale model for suspensions*, Discrete and Continuous Dynamical Systems - Series B **6** (2006), 449–470.

[54] I. Catto, C. Le Bris, and P.-L. Lions, **Mathematical theory of thermodynamic limits: Thomas-Fermi type models**, Oxford University Press (1998).

[55] C. Chauvière and A. Lozinski, *Simulation of dilute polymer solutions using a Fokker-Planck equation*, Computers and fluids, **33** (2004), 687–696.

[56] M. Chipot and D. Kinderlehrer, *Equilibrium configurations of crystals*, Arch. Rat. Mech. Anal. **103** (1988), 237–277.

[57] Ph. G. Ciarlet, **Mathematical elasticity**, volume 1, North Holland (1993).

[58] D. Cioranescu, P. Donato, **An introduction to homogenization.** Oxford Lecture Series in Mathematics and its Applications, 17. The Clarendon Press, Oxford University Press, New York, 1999.

[59] P. Constantin, *Nonlinear Fokker-Planck Navier-Stokes systems*, Commun. Math. Sci. **3** (2005), 531–544.

[60] P. Constantin, C. Fefferman, A. Titi, and A. Zarnescu, *Regularity of coupled two-dimensional nonlinear Fokker-Planck and Navier-Stokes systems*, Commun. Math. Phys. **270** (2007), 789–811.

[61] P. Constantin, I. Kevrekidis, and E.S. Titi, *Remarks on a Smoluchowski equation*, Disc. and Cont. Dyn. Syst. **11** (2004), 101–112.

[62] P. Constantin and N. Masmoudi, *Global well posedness for a Smoluchowski equation coupled with Navier-Stokes equations in 2D*, Commun. Math. Phys., **278** (2008), 179–191

[63] R. Costaouec, C. Le Bris, F. Legoll, *Approximation numérique d'une classe de problèmes en homogénéisation stochastique*, [Numerical approximation of a class of problems in stochastic homogenization], C. R. Acad. Sci. Série I, **348**, p 99-103, 2010.

[64] R. Costaouec, C. Le Bris, F. Legoll, *Variance reduction in stochastic homogenization: proof of concept, using antithetic variables*, Bol. Soc. Esp. Mat. Apl., 50, pp 9-27, 2010.

[65] R. Costaouec, Thèse de l' Université Paris Est, Ecole des Ponts, in preparation.

[66] P. Delaunay, A. Lozinski, and R.G. Owens, *Sparse tensor-product Fokker-Planck-based methods for nonlinear bead-spring chain models of dilute polymer solutions*, CRM Proceedings and Lecture Notes, Volume 41, 2007.

[67] M. Dobson and M. Luskin, *Analysis of a force-based quasicontinuum approximation,* Math. Mod. Num. Anal. **42** (2008), 113–139.

[68] M. Dobson and M. Luskin, *Iterative solution of the quasicontinuum equilibrium equations with continuation,* Journal of Scientific Computing **37** (2008), 19–41.

[69] M. Dobson and M. Luskin, *An analysis of the effect of ghost force oscillation on quasicontinuum error,* Math. Mod. Num. Anal. **43** (2009), 591–604.

[70] M. Dobson, M. Luskin, *An optimal order error analysis of the one-dimensional quasicontinuum approximation*, SIAM J. Numer. Anal. **47** (2009), 2455–2475.

[71] M. Dobson, M. Luskin, and C. Ortner, *Stability, Instability, and Error of the Force-based Quasicontinuum Approximation*, arXiv preprint 0903.0610.

[72] M. Dobson, M. Luskin, C. Ortner, *Sharp stability estimates for the accurate prediction of instabilities by the quasicontinuum method*, arXiv preprint 0905.2914.

[73] M. Doi and S.F. Edwards, **The Theory of Polymer Dynamics**, International Series of Monographs on Physics. Oxford University Press, 1988.

[74] W. E, T. Li, and P.W. Zhang, *Convergence of a stochastic method for the modeling of polymeric fluids*, Acta Mathematicae Applicatae Sinica, English Series, **18** (2002), 529–536.

[75] W. E, T. Li, and P.W. Zhang, *Well-posedness for the dumbbell model of polymeric fluids*, Commun. Math. Phys. **248** (2004), 409–427.

[76] B. Engquist and P. Souganidis,*Asymptotic and numerical homogenization*, Acta Numer. 17 (2008).

[77] Y. Efendiev and T. Hou, **Multiscale Finite Element method**, Theory and applications. Surveys and Tutorials in the Applied Mathematical Sciences, 4. Springer, New York, 2009.

[78] A. Ern and T. Lelièvre, *Adaptive models for polymeric fluid flow simulation*, C. R. Acad. Sci. Paris, Ser. I, **344** (2007), 473–476.

[79] J. Fang and R.G. Owens, *Numerical simulations of pulsatile blood flow using a new constitutive model*, Biorheology **43** (2006), 637–770.

[80] E. Fernández-Cara, F. Guillén, and R.R. Ortega, *Handbook of numerical analysis. Vol. 8: Solution of equations in* $\mathbb{R}^n$ *(Part 4). Techniques of scientific computing (Part 4). Numerical methods of fluids (Part 2).*, chapter Mathematical modeling and analysis of viscoelastic fluids of the Oldroyd kind, pages 543–661. Amsterdam: North Holland/ Elsevier, 2002.

[81] M.C. Fivel, C.F. Robertson, G.R. Canova and L. Boulanger, *Three-dimensional modeling of indent-induced plastic zone at a mesoscale*, Acta. Mater. **46** (1998), 6183–6194.

[82] I. Fonseca, *The lower quasiconvex envelope of the stored energy function for an elastic crystal*, J. Math. Pures Appl. **67** (1988), 175–195.

[83] I. Fonseca, *Variational methods for elastic crystals*, Arch. Rat. Mech. Anal. **97** (1987), 187–220.

[84] G. Forest, Q. Wang, and R. Zhou, *The flow-phase diagram of Doi-Hess theory for sheared nematic polymers II: finite shear rates*, Rheol. Acta **44** (2004), 80–93.

[85] G. Friesecke, R. D. James, and S. Müller, *Rigorous derivation of nonlinear plate theory and geometric rigidity*, C. R. Acad. Sci. Paris Sér. I, **334** (2002), 173–178.

[86] G. Friesecke and F. Theil, *Validity and failure of the Cauchy-Born hypothesis in a two-dimensional mass-spring lattice,* J. Nonlinear Sci., **12** (2002), 445–478.

[87] D. Gilbarg and N. S. Trudinger, **Elliptic partial differential equations of second order**, reprint of the 1998 ed., Classics in Mathematics. Berlin: Springer, 2001.

[88] A. Gloria, Reduction of the resonance error. Part 1: Approximation of homogenized coefficients, preprint available at `http://hal.archives-ouvertes.fr/inria-00457159/en/`.

[89] A. Gloria and F. Otto, An optimal error estimate in stochastic homogenization of discrete elliptic equations, preprint available at `http://hal.inria.fr/hal-00383953`.

[90] M. Grüter and K. O. Widman, The Green function for uniformly elliptic equations, *Manuscripta Math.* 37: 303–342, 1982.

[91] C. Guillopé and J.C. Saut, *Existence results for the flow of viscoelastic fluids with a differential constitutive law*, Nonlinear Analysis, Theory, Methods & Appl. **15** (1990), 849–869.

[92] C. Guillopé and J.C. Saut, *Global existence and one-dimensional nonlinear stability of shearing motions of viscoelastic fluids of Oldroyd type*, RAIRO Math. Model. Num. Anal. **24** (1990), 369–401.

[93] G. H. Hardy, J. E. Littlewood and G. Pólya, **Inequalities**, 2nd ed., 1st. paperback ed. Cambridge University Press. 1988.

[94] Hall, P. and Heyde, C. C., **Martingale limit theory and its application**, Probability and Mathematical Statistics. Academic Press, Inc., New York-London, 1980.

[95] P. Hébraud and F. Lequeux, *Mode-coupling theory for the pasty rheology of soft glassy materials*, Phys. Rev. Lett. **81** (1998), 2934–2937.

[96] `FreeFEM, http://www.freefem.org`

[97] U. Hornung, Chapter 1 of **Homogenization and Porous Media** Interdisciplinary Applied Mathematics, Springer.

[98] D. Hu and T. Lelièvre, *New entropy estimates for the Oldroyd-B model, and related models*, Commun. Math. Sci. **5** (2007), 909–916.

[99] V. V. Jikov, S. M. Kozlov, O. A. Oleinik, **Homogenization of differential operators and integral functionals,** Springer-Verlag, 1994.

[100] U. Krengel, **Ergodic theorems**, de Gruyter Studies in Mathematics, vol. 6, de Gruyter, 1985.

[101] F. John, *Rotation and strain*, Comm. Pure Appl. Math. **14** (1961), 391–413.

[102] F. John, *Bounds for deformations in terms of average strains*, in: Shisha O. (Ed.), Inequalities III, pp. 129–144, 1972.

[103] B. Jourdain, C. Le Bris, and T. Lelièvre, *On a variance reduction technique for micro-macro simulations of polymeric fluids*, J. Non-Newtonian Fluid Mech. **122** (2004), 91–106.

[104] B. Jourdain, C. Le Bris, T. Lelièvre, and F. Otto, *Long-time asymptotics of a multiscale model for polymeric fluid flows*, Arch. Rat. Mech. Anal. **181** (2006), 97–148.

[105] B. Jourdain and T. Lelièvre, *Mathematical analysis of a stochastic differential equation arising in the micro-macro modelling of polymeric fluids* In I.M. Davies, N. Jacob, A. Truman, O. Hassan, K. Morgan, and N.P. Weatherill, editors, "Probabilistic Methods in Fluids Proceedings of the Swansea 2002 Workshop", pages 205–223. World Scientific, 2003.

[106] B. Jourdain, T. Lelièvre, and C. Le Bris, *Numerical analysis of micro-macro simulations of polymeric fluid flows: a simple case*, Math. Models and Methods in Applied Sciences **12** (2002), 1205–1243.

[107] B. Jourdain, T. Lelièvre, and C. Le Bris, *Existence of solution for a micro-macro model of polymeric fluid: the FENE model*, Journal of Functional Analysis **209** (2004), 162–193.

[108] B. Jourdain, T. Lelièvre, and C. Le Bris, *Coupling PDEs and SDEs: the illustrative example of the multiscale simulation of viscoelastic flows*, in "Multiscale Methods in Science and Engineering", B. Engquist, P. Lötstedt, O. Runborg, eds., Lecture Notes in Computational Science and Engineering 44, Springer, 2005, pp 149-168.

[109] J. B. Keller and D. Givoli, *Exact nonreflecting boundary conditions,* J. Comput. Phys., **82** (1989), 172–192.

[110] R. Keunings, *Simulation of viscoelastic fluid flow*, in "Fundamentals of Computer Modeling for Polymer Processing", C. Tucker ed., Hanser, 1989, pp 402–470.

[111] R. Keunings, *A survey of computational rheology*, In D.M. Binding et al., editor, "Proc. 13th Int. Congr. on Rheology", pages 7–14. British Society of Rheology, 2000.

[112] D. Kinderlehrer, *Remarks about equilibrium configurations of crystals*, in "Material instabilities in continuum mechanics and related mathematical problems" (J. M. Ball, ed.), Oxford University Press, pp 217–242, 1998.

[113] D.J. Knezevic and E. Süli, *Spectral Galerkin approximation of Fokker-Planck equations with unbounded drift*, Math. Mod. Num. Anal. (M2AN), **43** (2009), 445–485.

[114] D.J. Knezevic and A.T. Patera, *A certified reduced basis method for the Fokker-Planck equation of dilute polymeric fluids: FENE dumbbells in extensional flow*, to appear in SIAM Journal on Scientific Computing.

[115] M. Laso and H.C. Öttinger, *Calculation of viscoelastic flow using molecular models: the CONNFFESSIT approach*, J. Non-Newtonian Fluid Mech. **47** (1993), 1–20.

[116] C. Le Bris, *Some numerical approaches for "weakly" random homogenization*, to appear in Proceedings of ENUMATH 2009, Springer Lecture Notes in Computational Science and Engineering.

[117] C. Le Bris, **Systèmes multiéchelles: modélisation et simulation**, *Mathématiques et Applications*, volume 47, Springer, 2005, ISBN: 3-540-25313-0.

[118] C. Le Bris et al., *Introduction to numerical stochastic homogenization and related computational challenges: some recent developments*, in preparation for Lecture Notes Series, Institute for Mathematical Sciences, National University of Singapore.

[119] C. Le Bris, in preparation with A. Gloria.

[120] C. Le Bris and P.L. Lions, *Renormalized solutions to some transport equations with partially $W^{1,1}$ velocities and applications*, Annali di Matematica pura ed applicata **183** (2004), 97–130.

[121] C. Le Bris and P.L. Lions, *Existence and uniqueness of solutions to Fokker-Planck type equations with irregular coefficients*, Comm. Part. Diff. Eq. **33** (2008), 1272–1317.

[122] F. Legoll, *Multiscale methods coupling atomistic and continuum mechanics: some examples of mathematical analysis*, in "Analytical and Numerical Aspects of Partial Differential Equations", E. Emmrich and P. Wittbold eds., de Gruyter Proceedings in Mathematics, pp 193-245, 2009.

[123] C. Le Bris and T. Lelièvre, *Multiscale modelling of complex fluids: a mathematical initiation*, in "Multiscale Modeling and Simulation in Science", Lecture Notes in Com-

putational Science and Engineering , Vol. 66, B. Engquist, P. Lötstedt, O. Runborg Eds., 2009, ISBN: 978-3-540-88856-7.

[124] C. Le Bris, T. Lelièvre, and Y. Maday, *Results and questions on a nonlinear approximation approach for solving high-dimensional partial differential equations*, Constructive Approximation **30** (2009), 621–651.

[125] T. Li, H. Zhang, and P.W. Zhang, *Local existence for the dumbbell model of polymeric fluids*, Comm. Part. Diff. Eq. **29** (2004), 903–923.

[126] T. Li and P.W. Zhang, *Convergence analysis of BCF method for Hookean dumbbell model with finite difference scheme*, SIAM MMS **5** (2006), 205–234.

[127] F.-H. Lin, C. Liu, and P.W. Zhang, *On hydrodynamics of viscoelastic fluids*, Comm. Pure Appl. Math. **58** (2005), 1437–1471.

[128] F.-H. Lin, C. Liu, and P.W. Zhang, *On a micro-macro model for polymeric fluids near equilibrium*, Comm. Pure Appl. Math. **60** (2007), 838–866.

[129] F.-H. Lin, P. Zhang, and Z. Zhang, *On the global existence of smooth solution to the 2-D FENE dumbell model*, Commun. Math. Phys. **277** (2008), 531-553.

[130] P.L. Lions and N. Masmoudi, *Global solutions for some Oldroyd models of non-Newtonian flows*, Chin. Ann. Math., Ser. B, **21** (2000), 131–146.

[131] P.L. Lions and N. Masmoudi, *Global existence of weak solutions to micro-macro models*, C. R. Math. Acad. Sci. **345** (2007), 15–20.

[132] P.L. Lions and P. Souganidis, *Homogenization of viscous Hamilton-Jacobi equations in stationary ergodic media*, Com. PDE, 30, 2005, 1-3, 335–375.

[133] A. Lozinski, "Spectral methods for kinetic theory models of viscoelastic fluids", PhD thesis, Ecole Polytechnique Fédérale de Lausanne, 2003, available at `http://library.epfl.ch/theses/?nr=2860`.

[134] A. Lozinski and C. Chauvière, *A fast solver for Fokker-Planck equation applied to viscoelastic flows calculations*, J. Comp. Phys. **189** (2003), 607–625.

[135] M. Luskin and C. Ortner, *An analysis of node-based cluster summation rules in the quasicontinuum method*, SIAM J. Numer. Anal. **47** (2009), 3070-3086.

[136] L. Machiels, Y. Maday, and A.T. Patera, *Output bounds for reduced-order approximations of elliptic partial differential equations*, Comput. Methods Appl. Mech. Engrg. **190** (2001), 3413–3426.

[137] N. Masmoudi, *Well posedness for the FENE dumbbell model of polymeric flows*, Comm. Pure Appl. Math. **61** (2008), 1685-1714.

[138] N. Masmoudi, *Global existence of weak solutions to the FENE dumbbell model of polymeric flows*, `http://arxiv.org/pdf/1004.4015v1.pdf`, preprint.

[139] R. Miller and E. B. Tadmor, *The Quasicontinuum Method: Overview, applications and current directions,* Journal of Computer-Aided Materials Design, **9** (2002), 203–239.

[140] R. Miller, E. B. Tadmor, R. Phillips, and M. Ortiz, *Quasicontinuum simulation of fracture at the atomic scale*, Modelling Simul. Mater. Sci. Eng. **6** (1998), 607.

[141] C. B. Morrey, Jr *Quasi-convexity and the lower semi-continuity of multiple integrals,* Pacific J. Math., **2** (1952), 25–53.

[142] S. Müller, *Variational models for microstructure and phase transitions*, in "Calculus of variations and Geometric evolution problems", Lecture Notes in Math. volume 1713, pp 85–210. Springer Verlag, Berlin, 1999.

[143] F. Murat, *Compacité par compensation*, Ann. Scuola Norm. Sup. Pisa. Cl. Sci. **5** (4) pp 485–507, 1978.

[144] A. Naddaf and T. Spencer, Estimates on the variance of some homogenization problems, preprint.

[145] D.P. Nicholls and N. Nigam, *Exact non-reflecting boundary conditions on general domains,* J. Comput. Phys. **194** (2004), 278–303.

[146] G. Nguetseng, *A general convergence result for a functional related to the theory of homogenization*, SIAM J. Math. Anal. **20** (3), pp 608-623, 1989.

[147] G. Nguetseng, *Homogenization structures and applications I*, Z. Anal. Anwendungen **22** (1), pp 73–107, 2003.

[148] G. Nguetseng, *Homogenization Structures and Applications II*, Zeitschrift für Analysis und ihre Anwendungen, **23**, No. 3, pp 483- 508, 2004.

[149] G. Nguetseng, *Almost periodic homogenization: asymptotic analysis of a second order elliptic equation*, preprint, unpublished, 2000.

[150] G. Nguetseng, *Homogenization of perforated domains beyond the periodic setting*, J. Math. Anal. Appl., **289**, pp 608-628, 2004.

[151] H.C. Öttinger, **Stochastic Processes in Polymeric Fluids**, Springer, 1995.

[152] R.G. Owens, *A new microstructure-based constitutive model for human blood*, J. Non-Newtonian Fluid Mech. **140** (2006), 57–70.

[153] R.G. Owens and T.N. Phillips, **Computational rheology**, Imperial College Press / World Scientific, 2002.

[154] G. Papanicolaou and S. R. S. Varadhan, *Boundary value problems with rapidly oscillating random coefficients*. In Proc. Colloq. on Random Fields: Rigorous Results in Statistical Mechanics and Quantum Field Theory (J. Fritz, J. L. Lebaritz and D. Szasz, eds), Vol. 10 of Colloquia Mathematica Societ. Janos Bolyai, pp. 835-873.

[155] G. Papanicolaou and S. R. S. Varadhan, *Diffusions with random coefficients*, Statistics and probability: essays in honor of C. R. Rao, pp. 547–552, North-Holland, Amsterdam, 1982.

[156] P. Pedregal, **Parametrized measures and variational principles**, Birkhäuser, 1997.

[157] M. Renardy, *Local existence of solutions of the Dirichlet initial-boundary value problem for incompressible hypoelastic materials*, SIAM J. Math. Anal. **21** (1990), 1369–1385.

[158] M. Renardy, *An existence theorem for model equations resulting from kinetic theories of polymer solutions*, SIAM J. Math. Anal. **22** (1991), 313–327.

[159] M. Renardy, **Mathematical analysis of viscoelastic flows**, CBMS-NSF Conference Series in Applied Mathematics 73, SIAM 2000.

[160] Y. G. Reshetnyak, *Liouville's theory on conformal mappings under minimal regularity assumptions*, Sibirskii Math. **8** (1967), 69–85.

[161] S. Sakata, F. Ashida, T. Kojima, and M. Zako, Three-dimensional stochastic analysis using a perturbation-based homogenization method for elastic properties of composite material considering microscopic uncertainty, *Int. J. Solids and Structures*, 45:894–907, 2008.

[162] V. B. Shenoy, R. Miller, E.B. Tadmor, R. Phillips, and M. Ortiz, *Quasicontinuum models of interfacial structure and deformation*, Phys. Rev. Lett. **80** (1998), 742.

[163] V. B. Shenoy, R. Miller, E.B. Tadmor, D. Rodney, R. Phillips, and M. Ortiz, *An adaptative finite element approach to atomic-scale mechanics - the QuasiContinuum Method*, J. Mech. Phys. Solids **47** (1999), 611.

[164] T. Shimokawa, J. Mortensen, J. Shiotz, and K. Jacobsen, *Matching conditions in the quasicontinuum method : removal of the error introduced at the interface between the coarse-grained and fully atomistic regions,* Phys. Rev. B **69** (2004), 214104.

[165] A. N. Shiryaev, **Probability**, Graduate Texts in Mathematics, vol. 95, Springer, 1984.

[166] P. Souganidis, *Recent developments in the theory of homogenization for fully nonlinear first- and second-order PDE in random environments*, Bol. Soc. Esp. Mat. Apl. SEMA, 34, 2006, 81–90.

[167] J.K.C. Suen, Y.L. Joo, and R.C. Armstrong, *Molecular orientation effects in viscoelasticity*, Annu. Rev. Fluid Mech. **34** (2002), 417–444.

[168] E.B. Tadmor, M. Ortiz, and R. Phillips, *Quasicontinuum analysis of defects in solids*, Phil. Mag. A, **73** (1996), 1529-1563.

[169] E.B. Tadmor and R. Phillips, *Mixed Atomistic and Continuum Models of Deformation in Solids*, Langmuir **12** (1996), 4529.

[170] E.B. Tadmor, G.S. Smith, N. Bernstein, and E. Kaxiras, *Mixed finite element and atomistic formulation for complex crystals*, Phys. Rev. B **59** (1999), 235.

[171] L. Tartar, *Compensated compactness and applications to partial differential equations,* Nonlinear analysis and mechanics: Heriot-Watt Symposium, Vol. IV, pp. 136–212, Res. Notes in Math., 39, Pitman, Boston, Mass.-London, 1979.

[172] L. Tartar, H-measures and small amplitude homogenization, in *Random media and composites*, Proc. SIAM Workshop, Leesburg/VA (USA) 1988, 89–99, 1989.

[173] L. Tartar, H-measures, a new approach for studying homogenisation, oscillations and concentration effects in partial differential equations, *Proc. R. Soc. Edinb., Sect. A*, 115(3-4):193–230, 1990.

[174] F. L. Teixeira and W. C. Chew, *Complex space approach to perfectly matched layers: a review and some new developments,* Int. J. Numer. Model. **13** (2000), 441-455.

[175] M. Thomas, *Propriétés thermiques de matériaux composites : caractérisation expérimentale et approche microstructurale*, [Thermal properties of composite materials: experimental characterization and microstructural approach], Thèse de l' Université de Nantes, Laboratoire de Thermocinétique, CNRS - UMR 6607, 2008.

[176] F. Thomines, Thèse de l' Université Paris Est, Ecole des Ponts, in preparation.

[177] T. von Petersdorff and C. Schwab, *Numerical solution of parabolic equations in high dimensions*, M2AN Math. Model. Numer. Anal. **38** (2004), 93–127.

[178] L. C. Young, **Lectures on the calculus of variations and optimal control theory**, W. B. Saunders Co., Philadelphia-London-Toronto, 1969.

[179] V. V. Yurinskii, Averaging of symmetric diffusion in random medium, *Sibirskii Mat. Zh.*, 27(4):167–180, 1986.

[180] H. Zhang and P.W. Zhang, *A theoretical and numerical study for the rod-like model of a polymeric fluid*, Journal of Computational Mathematics **22** (2004), 319–330.

[181] H. Zhang and P.W. Zhang, *Local existence for the FENE-dumbbell model of polymeric fluids*, Archive for Rational Mechanics and Analysis **2** (2006), 373–400.

[182] L.Y. Zhang, H. Zhang, and P.W. Zhang, *Global existence of weak solutions to the regularized Hookean dumbbell model*, Comm. Math. Sci. **6** (2008), 85-124.